ELSEVIER

Contents lists available at ScienceDirect

Journal of Plant Physiology

journal homepage: www.elsevier.com/locate/jplph





Genotype-specific nonphotochemical quenching responses to nitrogen deficit are linked to chlorophyll *a* to b ratios

Seema Sahay a,b, Marcin Grzybowski b,c,d, James C. Schnable b,c, Katarzyna Głowacka a,b,e,*

- ^a Department of Biochemistry, University of Nebraska-Lincoln, Lincoln, NE, USA
- b Center for Plant Science Innovation, University of Nebraska-Lincoln, Lincoln, NE, USA
- ^c Department of Agronomy and Horticulture, University of Nebraska-Lincoln, Lincoln, NE, USA
- d Department of Plant Molecular Ecophysiology, Faculty of Biology, Institute of Plant Experimental Biology and Biotechnology, University of Warsaw, 02-096 Warsaw, Poland
- e Institute of Plant Genetics, Polish Academy of Sciences, 60-479, Poznań, Poland

ARTICLE INFO

Keywords:
Non-photochemical quenching
Natural variation
Maize
Nitrogen
Phenotypic plasticity

ABSTRACT

Non-photochemical quenching (NPQ) protects plants from photodamage caused by excess light energy. Substantial variation in NPQ has been reported among different genotypes of the same species. However, comparatively little is known about how environmental perturbations, including nutrient deficits, impact natural variation in NPO kinetics. Here, we analyzed a natural variation in NPO kinetics of a diversity panel of 225 maize (Zea mays L.) genotypes under nitrogen replete and nitrogen deficient field conditions. Individual maize genotypes from a diversity panel exhibited a range of changes in NPQ in response to low nitrogen. Replicated genotypes exhibited consistent responses across two field experiments conducted in different years. At the seedling and pre-flowering stages, a similar portion of the genotypes (~33%) showed decrease, no-change or increase in NPQ under low nitrogen relative to control. Genotypes with increased NPQ under low nitrogen also showed greater reductions in dry biomass and photosynthesis than genotypes with stable NPQ when exposed to low nitrogen conditions. Maize genotypes where an increase in NPQ was observed under low nitrogen also exhibited a reduction in the ratio of chlorophyll a to chlorophyll b. Our results underline that since thermal dissipation of excess excitation energy measured via NPQ helps to balance the energy absorbed with energy utilized, the NPQ changes are the reflection of broader molecular and biochemical changes which occur under the stresses such as low soil fertility. Here, we have demonstrated that variation in NPQ kinetics resulted from genetic and environmental factors, are not independent of each other. Natural genetic variation controlling plastic responses of NPQ kinetics to environmental perturbation increases the likelihood it will be possible to optimize NPQ kinetics in crop plants for different environments.

1. Introduction

The production and application of synthetic nitrogen (N) fertilizer have played a critical role in our civilization's ability to meet growing needs for food and fuel over the last century. Prior to the advent of synthetically produced biologically accessible forms of nitrogen, access to nitrogen was the rate-limiting factor on crop productivity in many environments. Today, the more than 118 million tons of N fertilizer per year used by the agricultural sector (FAO, 2019; Sandhu et al., 2021) is responsible for half the calories used to feed the world's population (Smil, 2001). However, the production of this fertilizer is energy

intensive (Giles, 2005; Hirel et al., 2007) and the application of N fertilizer to fields results in the production of nitrous oxide (N_2O) a greenhouse gas estimated to be 298 times more potent than CO_2 (Stulen et al., 1998; Baggs et al., 2006; Park et al., 2012). One of the crops which has benefited substantially from access to N fertilizer is maize (Duvick, 2005; USDA-NASS, 2017). Today many farmers apply nitrogen fertilizer to maize fields at rates in excess of 300 kg/ha/year (Zhang et al., 2015; Cao et al., 2018). The cost to farmers of nitrogen fertilizer can exceed \$300 ha/year ('Statista, 2022'; Rodríguez-Espinosa et al., 2023).

Given both the environmental and economic costs of excessive use of nitrogen fertilizer, there is growing interest in breeding maize varieties

^{*} Corresponding author. Department of Biochemistry, University of Nebraska-Lincoln, Lincoln, NE, USA.

E-mail addresses: ssahay2@unl.edu (S. Sahay), marcin.grzybowski@uw.edu.pl (M. Grzybowski), schnable@unl.edu (J.C. Schnable), kglowacka2@unl.edu (K. Głowacka).

that are more productive under nitrogen-limited conditions. However, there are many biological challenges which must be overcome to achieve this goal (Ciampitti et al., 2022). One of these challenges is that nitrogen deficit presents substantial challenges to maintaining plant photosynthetic productivity. Low N availability hinders the growth and development of plants at both physiological and molecular levels (Martin et al., 2002; Ding et al., 2005; Peng et al., 2007; Kant et al., 2008; Bi et al., 2009). Nitrogen deficiency accelerates leaf yellowing via chlorophyll degradation, anthocyanin accumulation and senescence which decreases the rate of CO2 assimilation and reduces soluble protein content (Ding et al., 2005; Diaz et al., 2006; Zhao et al., 2017), and leaf expansion rates and total leaf area (Monneveux et al., 2006; T. Liu et al., 2018b). In maize, inadequate N supply impairs ultrastructure and function of chloroplast by reducing the number of chloroplasts per cell, lamellae per grana, which weakens photosynthesis and decreases biomass and grain yield (Jin et al., 2015; Z. Liu et al., 2018a). The changes in leaf morphology and anatomy, as well as changes in chloroplast ultrastructure and the abundance of different photosynthetic pigments resulting from nitrogen deficit stress, impact the conditions under which critical photosynthetic processes including those which determine levels of non-photochemical quenching (NPQ) operates. The amount of light absorbed in plants often exceeds the capacity of the electron-transfer reactions (Pearcy, 1990; Burgess et al., 2016). Absorption of excess energy can lead to the production of damaging reactive oxygen species which can cause irreversible decline in photosynthetic efficiency (Müller et al., 2001). To prevent PSII from photodamage, plants employ a set of mechanisms to dissipate the excess energy absorbed by plant leaves. The dissipation of excess energy that results from these mechanisms can be quantified and is collectively referred to as NPQ. Transgenic interventions that produce more rapid changes in NPQ in response to changes in light intensity have been found to be associated with both greater photosynthetic capacity and biomass in tobacco, soybean, and rice (Kromdijk et al., 2016; De Souza et al., 2022; Xin et al., 2023) and reduced biomass and yield in Arabidopsis thaliana and potato (Garcia-Molina and Leister, 2020; Lehretz et al., 2022).

Previous studies have found extensive variation in the maximum level of NPQ observed in diverse populations of rice and Arabidopsis (Jung and Niyogi, 2009; Wang et al., 2017; Rungrat et al., 2019). We recently demonstrated that, under well fertilized field conditions over multiple years there is also significant, genetically-controlled variation in the NPO changes in response to sudden changes in light intensity which allowed us to identify distinct sets of genes controlling different attributes of the NPQ kinetics (Sahay et al., 2023). However, comparatively little is known about how environmental perturbations, including nutrient deficits, impact natural variation in NPQ kinetics. We quantified NPQ kinetics at multiple developmental stages across a maize association panel grown in the field under low- and control-N. We identified diverse patterns of response/non-response to nitrogen treatment which were validated, for a subset of genotypes, across multiple additional environments and linked to differences in both CO2 assimilation and growth. We identify specific changes to the photosynthetic apparatus that are associated with, and may explain, why some maize genetics exhibit large changes in NPQ kinetics in response to nitrogen deficit stress while others do not.

2. Materials and Methods

2.1. Field experiments with the maize association panel

A collection of 225 diverse maize accessions (hereafter referred to as genotypes) from the Buckler-Goodman maize association panel (Flint-Garcia et al., 2005) were evaluated in a field experiment in 2019 (Table S1). A subset of 47 genotypes from the same population were also planted in the field in 2020. Both field experiments were conducted under non nitrogen limiting (hereafter referred to as control) and

nitrogen limiting (hereafter referred to as low N) conditions at the University of Nebraska-Lincoln Havelock Research Farm, Lincoln, NE, USA. The 2019 field was located at N 40.853, W 96.611 and the 2020 field was located at: N 40.859, W 96.598.

The 2019 field experiment has been previously described by (Meier et al., 2022; Rodene et al., 2022). Briefly, a completely randomized block (CRB) design experiment was set up with four blocks on 1st June. Each block consisted of 252 plots with a complete set of 225 genotypes and a replicated genotype (B73 \times Mo17) included as a repeated check. Two blocks each were grown under control (54.43 kg/acre) and low N (no nitrogen applied) for a total of 1008 plots. Replicates of the control and low N blocks were arranged diagonally, with the two control blocks in the North-East and South-West corners of the field and two low N blocks in North-West and South-East corners of the field. Each block was surrounded by border plots to minimize edge effects. Plots from the entire experiment were positioned in a grid of 176 (North-East and South-West) by 15 (North-West and South-East) plots (Table S2).

In 2020, the subset of 47 genotypes was planted on 22nd May in a CRB design in 8 blocks of 52 plots each. Each block included the complete set of 47 genotypes with B97 as a repeated check. Four blocks were assigned to control treatment and four blocks were assigned to low N treatment. A one plot (two rows) wide border was planted around the complete experiment while control and low N blocks were separated by a two-plot-wide border. In this study, NPQ data were collected from a subset of 23 genotypes among the 47 genotypes planted. The field was laid out in a grid of 18 (East-West) by 30 (North-South) plots (Table S3).

In both years, plots consisted of two rows of the same genotype with a spacing of $\sim\!\!75$ cm between rows and $\sim\!\!15$ cm between sequential plants in the same row. In 2019, plots were 5.6-m long, with 38 kernels planted per row. In 2020, plots were 1.5-m long with 11 kernels planted per row. In both years, nitrogen fertilizer was applied in control plots in the form of urea prior to planting. No nitrogen was applied in low N plots. Standard agronomic practices were employed throughout the experiment to control the weeds.

2.2. Plant propagation in growth-chamber

The seeds were surface sterilized with 20% bleach for 20 min, followed by five times washing and overnight soaking in distilled water. Seeds were sown in 6-L pots (13008000, Hummert International, Earth City, MO, USA) filled with Metromix 200 soil mixture (BM2 Germination and Propagation Mix; Berger, Saint-Modeste, Canada) in growth chambers (PGC20, Conviron, Manitoba, Canada). Conditions in growth chambers were maintained at a 16-h photoperiod of 900 µmol m⁻² s⁻¹ light intensity, 25 °C/20 °C day/night temperature, and 65–70% relative humidity. In the preliminary experiment, four nitrogen treatments: control (210.2 mg of N L^{-1}), moderate (140 mg of N L^{-1}), low (105.1 mg of N L^{-1}) and insufficient N (25 mg of N L^{-1}) were tested on B73 maize genotype. After 4 days after germination, plants were irrigated with Hoagland media containing different nitrogen treatments twice a week, and soil was maintained with 90% field water capacity every day (for details about media composition see Supplementary Method 1). Based on the preliminary test on B73 maize genotype with four nitrogen treatments, low N treatment (105.1 mg of N L⁻¹) was used for further experiments in the growth chamber due to a significant but moderate effect on physiological traits ($P \le 0.04$; Fig. 1A–G) and biomass ($P \le$ 0.02; Fig. S1H). Oppositely, a small reduction in N (moderate N treatment i.e., 140 mg of N L-1) led only to non-significant differences from control, however lowering N amount to 25 mg of N $\rm L^{-1}$ Hoagland media (insufficient N treatment) showed very early on yellowing leaf phenotype suggesting severe N deficiency. For the growth chamber condition experiments four genotypes were chosen from the maize association panel to represent increased (Group A genotypes; MS153 and Mo1W) or no-change (Group B genotypes; NC312, and H100) in NPQmax under low N conditions.

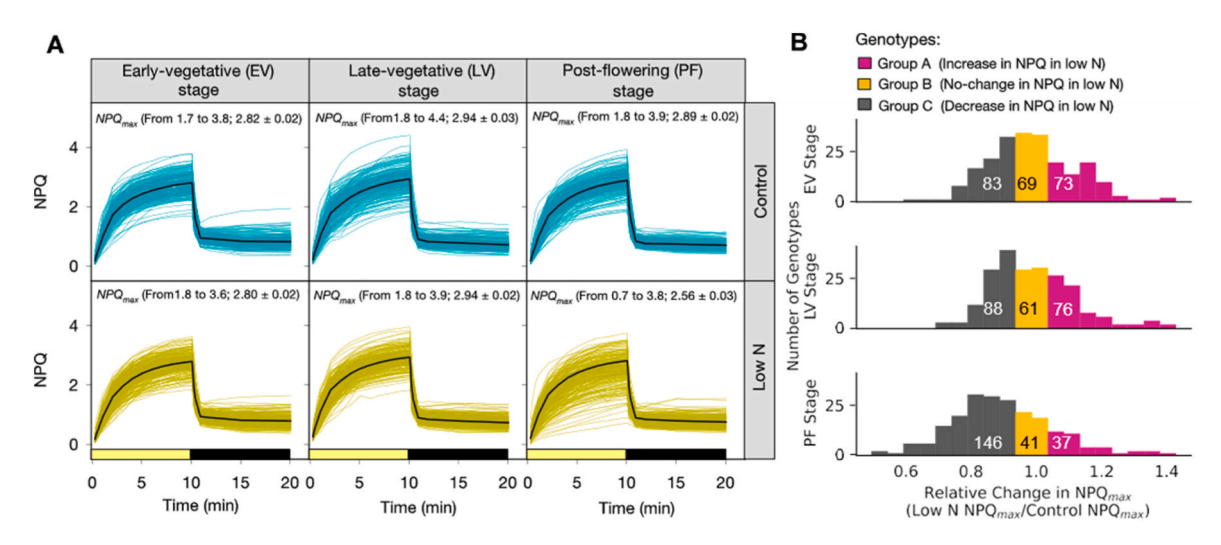


Fig. 1. Distribution of kinetics curves of nonphotochemical quenching (NPQ) and maximum value of NPQ (NPQ_{max}) at three developmental stages for maize (Z. mays) association panel grown in the field under control and low-nitrogen conditions. (A) NPQ induction and relaxation kinetics for 225 genotypes at early-vegetative (EV), late-vegetative (LV), and 224 at post-flowering (PF) stages measured in 2019 under control and low-N conditions. Each colored line represents the average value observed for an individual maize genotype across replicated plots of the same genotype in the same treatment and multiple leaf disks collected from each plot. Solid black lines indicate the overall mean NPQ response across all genotypes at a given developmental stage and treatment. The yellow horizontal bar indicates the timing of light treatment and the black horizontal bar represents the timing of the dark treatment. (B) Distribution of the relative changes in NPQ capacity of different maize genotypes under low nitrogen after 10 min of light treatment (NPQ_{max}) in maize genotypes at each of the three developmental stages evaluated. The numbers over the gray, orange, and pink indicate number of genotypes exhibiting a decrease (Group C; defined as $\leq 95\%$ of value from the control conditions), no change (Group B), and increase (Group A; defined as $\geq 105\%$ of corresponding control conditions) of the NPQ_{max} under low N relative to control conditions, respectively. Data used to produce this figure are given in Dataset 1. (For interpretation of the references to color in this figure legend, the reader is referred to the Web version of this article.)

2.3. Measuring NPQ kinetics for field-grown and growth-chamber-grown maize plants

NPQ kinetics were quantified for the maize association panel grown in the field, 26 d, 47 d and 66 d after sowing in 2019, and 33 d, 49 d, and 76 d after sowing in 2020. These timepoints corresponded to earlyvegetative (EV), late-vegetative (LV), and post-flowering (PF) stages, respectively. For each developmental stage, collection of data took four consecutive days. In 2019 and 2020, two and three plants from the middle of the row were analyzed per plot, respectively. For growthchamber-grown plants, the NPQ kinetics were measured 40 d after sowing, which corresponded to late vegetative stage. As previously described (Sahay et al., 2023), NPQ kinetics were investigated in semi-high-throughput manner on leaf disks (0.32 cm²) collected to the 96-well plates (781611; BrandTech Scientific, Essex, Ct, USA) from the sun exposed middle portion of the youngest fully expanded leaves. Leaf disks were cut using a hand-held puncher between 16:00 and 18:30 h, positioned with the adaxial surface facing down into plate, covered with moist sponges and incubated overnight in the dark. The following day disks were imaged using a modulated chlorophyll fluorescence imager (FluorCam FC 800-C, Photon Systems Instruments, Drasov, Czech Republic). First the minimum (F_0) and maximal (F_m) fluorescence in the dark were imaged. Subsequently, the leaf disks was subjected to 10 min of 2000 $\mu mol \; m^{-2} \; s^{-1}$ light (a combination of 1000 $\mu mol \; m^{-2} \; s^{-1}$ of a red-orange light with $\lambda max = 617$ nm and $1000 \ \mu mol \ m^{-2} \ s^{-1}$ of a cool white 6500 K light), corresponding to the highest light intensity experienced by field grown maize plants in Lincoln, Nebraska, followed by 10 min of darkness. To capture changes in steady state fluorescence (F_s) and maximum fluorescence under illuminated conditions (Fm') over time, the saturating flashes were provided at the following intervals (in
$$NPQ = F_m / F_m - 1$$
 Eqn. 1

The NPQ measured here mostly represents two of the fastest components of NPQ phenomenon, which are energy-dependent (qE) and zeaxanthin-dependent quenching (qZ) (Nilkens et al., 2010).

Maximum PSII efficiency (F_v/F_m) was estimated using following equation (Kitajima and Butler, 1975):

$$F_{v} / F_{m} = (F_{m} - F_{o}) / F_{m}$$
 Eqn. 2

2.4. Derivation of NPQ kinetics traits

The parameters attributed to rate, amplitude, and steady state of NPQ kinetics were obtained by fitting hyperbola and exponential equation to NPQ curves in the light (induction; Eqns. (3) and (4)), or in the darkness (relaxation; Eqns. (5) and (6); Table S4) using MATLAB (Matlab R2019b; MathWorks, Natick, MA, USA). The complete list of the eight analyzed parameters and their biological meanings are presented in Table S4. Goodness of fit was defined as the discrepancy between measured values and the values predicted by the equation fit to the data.

$$NPQ = \frac{time \times NPQslope_{lightH} + NPQasymptote_{lightH} - \sqrt{\left(time \times NPQslope_{lightH} + NPQasymptote_{lightH}\right)^2 - 4 \times 0.5 \times time \times NPQslope_{lightH} \times NPQasymptote_{lightH}}}{(2 \times 0.5)}$$

Eqn. 3

Eqn. 5

NPQ =
$$NPQasymptote_{lightE} \times \left(1 - exp^{\left(-NPQrate_constant_{light} \times time\right)}\right)$$
 Eqn. 4

data were analyzed with the PhotosynQ web application (https://photosynq.org). At late-vegetative stage of field (45-day-old) and growth chamber (35-days-old) grown plants, the transient value of theoretical NPQ (NPQ_T), based on assumption that F_{ν}/F_m is 0.83, was estimated

$$NPQ = NPQ start_{darkH} \\ - \frac{\left(time \times NPQ slope_{darkH} + NPQ amplitude_{darkH} - \sqrt{\left(time \times NPQ slope_{darkH} + NPQ amplitude_{darkH}\right)^2 - 4 \times 0.5 \times time \times NPQ slope_{darkH} \times NPQ amplitude_{darkH}}\right)}{(2 \times 0.5)}$$

$$NPQ = NPQ amplitude_{darkE} \times \left(exp^{(-NPQrate_constant_{dark} \times time)}\right) + NPQ residual_{dark}$$
 Eqn. 6

2.5. Data integrity and quality control Procedure

For data integrity analysis, each individual leaf disk measurement was subjected to two-stages of quality control (QC) process. The first stage involved assessing lower F_{ν}/F_m and the second stage was based on the goodness of fit for hyperbolic equations fitted to the measured NPQ. In the control treatment conditions, leaf disks with F_{ν}/F_m values lower than 0.58 were excluded. However, in low-N treatment conditions, no values were excluded, as the effects of low N on F_{ν}/F_m were taken into account. Measurements with poor fit (below the 1.5th percentile of the goodness of the fit) were excluded for both control and low N treatment conditions.

2.6. Broad sense heritability and percent genetic variation

To analyze the effects of genotype, nitrogen condition, developmental stage, and their interactions on each trait, a linear model followed by analysis of variance (ANOVA) was used. The following model was fit:

$$\label{eq:total_control_control} \begin{split} & Trait \sim Genotype + Nitrogen_Treatment + Development_Stage + \\ & Genotype*Nitrogen_Treatment + Genotype*Development_Stage + \\ & Development_Stage*Nitrogen_Treatment + Genotype*Development_Stage*Nitrogen_Treatment. \end{split}$$

The sum of squares (SS) for each term in the model was extracted and divided by the total SS to obtain the percentage of variance explained by each term. To calculate broad-sense heritability, a separate linear model was fitted for each trait for each treatment condition and developmental stage. The variance due to genotype divided by total variance was used as a broad-sense heritability estimate.

2.7. Fluorescence- and absorbance-based photosynthetic parameters

In 2020 field trial and growth-chamber experiments, fluorescence and absorbance-based parameters were measured on plants using spectrophotometers (MultispeQ V2.0; PhotosynQ, East Lansing, MI, USA; Kuhlgert et al., 2016). All the measurements were performed using Photosynthesis Rides protocol provided by the manufacturer, that is based on Pulse-Amplitude-Modulation (PAM) method and MultispeQ

from F_m ' and F_o ' using following equation (Tietz et al., 2017):

$$NPQ_T = \frac{4.88}{\left(\frac{F_{n_i}}{F_o} - 1\right)} - 1$$
 Eqn. 7

NPQ_T is a thermal dissipation parameter that was developed for measurements in the field that are hard to obtain in the dark. In our study, to reduce the chance of overestimating the NPQ_T the correction was performed using the actual F_{ν}/F_{m} of dark-adapted leaves estimated from fluorescence images of leaf disks. Quantum yields of photochemical quenching (Φ_{PSII}), non-photochemical quenching (Φ_{NPQ}), and other unregulated dissipation (Φ_{NO}) were calculated using Eqns. (8)–(10), respectively (Kuhlgert et al., 2016).

$$\Phi_{\text{PSII}} = \frac{F_m' - F_s'}{F_m'}$$
 Eqn. 8

$$\Phi_{NPO} = 1 - \Phi_{PSII} - \Phi_{NO}$$
 Eqn. 9

$$\Phi_{\text{NO}} = \frac{1}{NPQ_T + 1 + qL \times 4.88}$$
 Eqn. 10

Where, qL is the estimation of the fraction of open PSII centers using Stern-Volmer model.

In addition, in growth-chamber experiment leaf thickness based on Hall Effect and leaf relative chlorophyll content (Chl_{PQSPAD}) based on absorbance at 650 and 940 nm were measured using MultispeQ (Maas and Dunlap, 1989; Kuhlgert et al., 2016). Total electrochromic shift (ECS_T) was also estimated using the MultispeQ based on the Dark Interval Relaxation Kinetics (DIRK) method to monitor proton fluxes and the transthylakoid proton motive force (pmf) in vivo. This method is based on analyzing the ECS signals by fitting them to exponential decay curves provided estimations, related to the light-dark difference in thylakoid pmf (ECS_T). It was calculated according Eqn. (11) where tau (τ) is the relaxation time for the ECS signal, which is inversely related to the activity of the ATP synthase (Sacksteder et al., 2000).

$$ECS_T = \frac{ECS}{1 - e^{-\frac{1}{2}}}$$
 Eqn. 11

The proton conductivity (gH⁺) that is proportional to the aggregate conductivity of the thylakoid membrane to protons and largely dependent on the activity of ATP synthase was calculated after (Kanazawa and Kramer, 2002) using Eqn. (12).

$$gH^{+} = \frac{-1}{\tau}$$
 Eqn. 12

The redox state of photosystem I (PSI) reaction centers was estimated based on $P700^+$ absorbance changes at 810 and 940 nm to monitor active centers (PSI_{ac}), over-reduced center (PSI_{orc}), and oxidized center (PSI_{oxc}) after Klughammer and Schreiber (1994) and Kanazawa et al. (2017).

All the measurements were performed on the youngest fully expanded leaf. In the field, three randomly selected plants from the middle of the row of each plot were measured per genotype.

2.8. Photosynthetic gas exchange and fluorescence measurements

Photosynthetic gas exchange measurements were performed on the youngest fully developed leaf of the growth-chamber-grown plants at late-vegetative stage (37 days after germination) using a LI-6800 equipped with an integrated modulated fluorometer (LI-COR, Inc. Lincoln, NE, USA). Pulse amplitude-modulated chlorophyll fluorescence measurements were used with the multiphase flash routine (Loriaux et al., 2013). The fluorescence was measured in parallel with gas exchange measurements under steady state and fluctuating light to determine the light (Q) response of leaf net CO₂ assimilation (A_n), linear electron transport (J), photosystem II operating efficiency (Φ_{PSII}) and NPQ. The [CO₂] inside the cuvette, block temperature and water vapor pressure deficit were controlled at 400 μmol mol⁻¹, 23 °C, and 1.3 kPa, respectively. Leaf was dark adapted for 20 min in 6 cm² cuvette after which F_0 and F_m values were recorded to calculate F_{ν}/F_m (Eqn. (2)). For steady state measurements, light intensity was gradually increased from 0 to 25, 50, 75, 100, 125, 150, 200, 400, 600, 800, 1000, 1400, 1800 and 2000 μ mol m⁻² s⁻¹. A_n , stomatal conductance (g_s), F_s and F_m ' data were simultaneously recorded when reached steady state at each step which lasted between 300 and 600 s. For fluctuating light response measurements, the leaf first adapted to 2000 μ mol m⁻² s⁻¹ to reach steady-state of gas exchange, then the light intensity was varied from 2000 to 1800, 1400, 1000, 800, 600, 400, 200, 150, 125, 100, 75, 50, and 25 $\mu mol\ m^{-2}$ $\rm s^{-1}$. Each step lasted 4 min and was followed by 2000 μ mol m⁻² s⁻¹ for 4 min. At each light intensity, gas exchange and fluorescence data were recorded three times with 80 s interval between these measurements. The average values of three measurements recorded in 80 s intervals at each light intensity were used to reconstruct the final light response curve per each biological replicate.

For both light response curves J were calculated according to Eqn. (13).

$$J = 0.843 \times \Phi PSII \times PFD \times 0.5$$
 Eqn. 13

Quantum efficiency of CO_2 assimilation (ΦCO_{2max}) and quantum efficiency of linear electron transport ($\Phi PSII_{max}$) were derived from initial slope of the non-rectangular hyperbola equation fit to the lightresponse (Q) curves of A_n and J, respectively. A_{sat} and J_{max} were obtained from the asymptote of the non-rectangular hyperbola equation fit to A_n/Q and J/Q curves, respectively.

To measure CO_2 response to A_n (A/C_i curve), leaves were clumped in the cuvette in which light, [CO₂], block temperature and water vapor pressure deficit were controlled at 2000 µmol m⁻² s⁻¹, 400 µmol mol⁻¹, 23 °C, and 1.3 kPa, respectively. After the leaf reached steady-state of gas exchange, the CO_2 concentrations in the cuvette was varied from 400 to 50, 100, 150, 250, 350, 400, 500, 700, 900, and 1200 µmol mol⁻¹. Gas exchange parameters were recorded when steady state was reached in each step. Non-rectangular hyperbola was fit to A_n response to intracellular CO_2 concentration (C_i) to obtain *in vivo* capacity for phosphoenol-pyruvate (PEP) carboxylation (V_{pmax} ; initial slope) and capacity for PEP regeneration and leakage of CO_2 from the bundle sheath which determine the [CO_2]-saturated rate of A_n (V_{max} ; asymptote of the curve) ($C_{aemmerer}$ von, 2000).

2.9. Photosynthesis-related pigments quantification

After 42 d since sowing, $0.635~\rm cm^2$ of leaf tissue was collected from the youngest fully expanded leaf of the growth-chamber- and field-grown plants 4 h after the start of photoperiod. Tissue was ground in liquid nitrogen and combined with 500 μ l of pre-chilled 90% methanol (A452-1, Fisher Scientific, Hampton, NH, USA) vortexed and finally incubated for 4h on ice. The mixture was centrifuged for 5 min at $1902\times g$ at 4 °C (5424R, Eppendorf, Enfield, CT, USA) and pellet washed with additional methanol until it became completely white. Supernatant was transferred to 96-well plates to measure the absorbance at 470, 652 and 665 nm using a plate reader (Microplate Reader HT, Bio Tek, Winooski, VT, USA). Chlorophyll (Chl) a,b and total carotenoid contents were determined using the measured absorptions and the equations of (Lichtenthaler, 1987).

2.10. Analysis of growth and morphological traits

After 42 d since sowing the growth chamber growing plants were harvested to estimate leaf area, total fresh weight, and stalk height. The pictures of separate leaves were analyzed in ImageJ (National Institute of Health, Maryland, USA) to obtain a total leaf area. To evaluate the dry weight of above and below ground fraction of plants the roots, leaves and stalk were dried to constant weight at 60 $^{\circ}$ C. In addition, the specific leaf area was calculated as the ratio of leaf area to leaf dry mass (Garnier et al., 2001).

2.11. Statistical analysis

All statistical analysis of NPQ kinetics measurements was performed using SAS (version 9.4, SAS Institute Inc., Cary, NC, USA). Normal distribution and homogeneity of variance in data were tested with the Shapiro–Wilk and the Brown–Forsythe test, respectively. When either test rejected the null hypothesis, data was transformed and the tests were rerun. If one or both tests still rejected the null hypothesis the Wilcoxon non-parametric test was used in place of statistical tests which assume normal distributions. For data where both statistical tests failed to reject the null hypothesis, significant effects of treatment and genotype were evaluated using two-way ANOVA ($\alpha=0.05$) followed by Dunnett's test or two-tailed Student t-test to address the comparison of low N treatment to control treatments. Mean values for each genotype in each treatment or stage were employed in estimates of Pearson correlation.

3. Results

3.1. Variation in NPQ kinetics across three developmental stages and two nitrogen treatments in 225 maize genotypes

A semi-high-throughput method based on fluorescence assay of leaf disks collected to 96-well plates (Sahay et al., 2023) was used to quantify the NPQ kinetics in leaf disks collected from a field experiment consisting of a maize association panel grown under two nitrogen treatments with replication. In 2019, a combined total of 6002 leaf disks were collected across three time points from a maize field experiment with replicated genotypes grown under both control and low-nitrogen conditions. Data for 5796 disks passed quality control and were employed in downstream analyses, providing information on the response of 225 diverse maize genotypes at the early vegetative (EV) and the late vegetative (LV) stage and 224 diverse maize genotypes at the post-flowering (PF) stages. Substantial variation in the kinetics of NPQ were observed among the genotypes at each developmental stage and under each treatment (Fig. 1A). The maximum NPQ over the 10-min high-light period (NPQmax), one of the most widely reported parameters of the NPQ phenomenon, showed a similar range from 1.7 to 4.4 (average of 2.9) at five of the six combinations of developmental stages

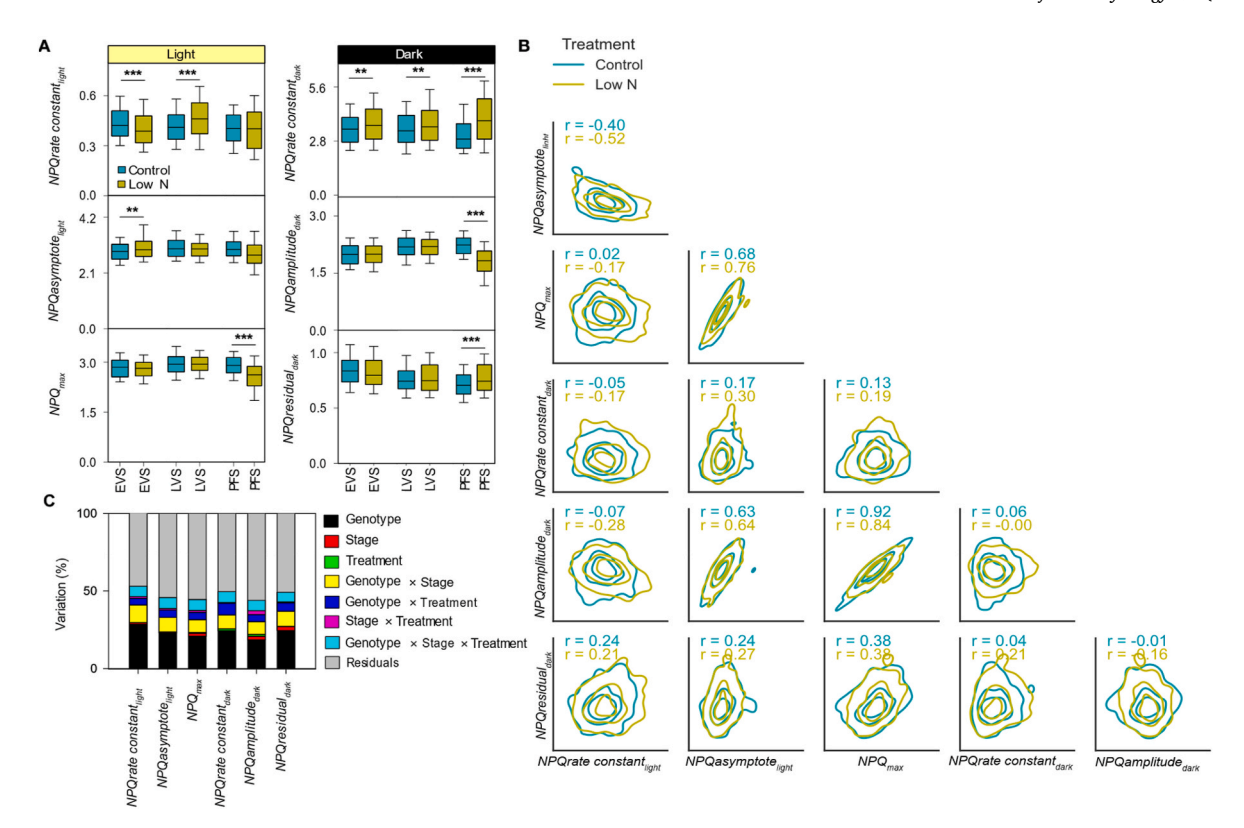


Fig. 2. Variation in NPQ kinetics traits among N treatments in three developmental stages and correlation between NPQ traits in late-vegetative stage for maize (Z. mays) association panel grown in the field. (A) Differences in the population-level distributions of different traits describing specific attributes of NPQ kinetics. The speed of NPQ induction in the light and NPQ relaxation in the dark are described by $NPQarate constant_{light}$ and $NPQrate constant_{dark}$, respectively. Steady-state NPQ under high light and steady-state NPQ in the dark after relaxation are described by $NPQarate constant_{light}$ and $NPQrate constant_{dark}$, respectively. The range of NPQ relaxation is described by $NPQamplitude_{dark}$, NPQ_{max} is the last value of NPQ in light (a full definition of each trait is provided in Table S4). The central line within each box plot indicates the median; the extent of the box indicates the 25th and 75th percentile values; upper and lower whiskers show either the minimum and maximum value or $1.5 \times \text{interquartile range}$, whichever results in a shorter whisker (n = from 224 to 225 genotypes). (B) Correlations among the six traits describing the attributes of NPQ kinetics at the late-vegetative stage. Contour lines in each plot indicate the density of maize genotypes for a pair of phenotypes under the two nitrogen treatments. Separate Pearson's correlation coefficients (r) are displayed in each panel for each of the two N treatments. (C) The percentage of variance explained by three factors (genotype, stage, treatment) and the percentage of variance explained by the interactions between these three factors for six traits describing attributes of NPQ kinetics for association panel grown in the field. In panel A and B, asterisks indicate significant differences between control and low N (paired t-test; $*P \le 0.05$; $**P \le 0.01$; $***P \le 0.001$). Data used to produce this figure are given in Dataset 1.

and treatments (Fig. 1A). The exception was the PF stage under low N in which plants showed much lower values of NPQ_{max} that extended substantially the range of this trait from 0.7 to 3.8 (average of 2.6). Based on change in NPQ_{max} between treatments, maize genotypes were sorted into three groups: genotypes where NPQ_{max} increased under low-nitrogen conditions relative to control (Group A), genotypes where NPQ_{max} did not change in response to nitrogen treatment (Group B) and genotypes where NPQ_{max} decreased under low-nitrogen conditions relative to control (Group C). At the early- and late-vegetative stages a similar fraction of genotypes belonged to each of these three groups. However, at the late-developmental stage when our nitrogen deficit treatment should produce the most severe stress, 64% of genotypes exhibited decreases in NPQ_{max} under low-N-treatment (Fig. 1B).

In addition to NPQ_{max} we also considered a set of six traits extracted from NPQ response curves that quantify the rate, steady state, and range of the NPQ response to light and dark in individual leaf samples. Significant differences between control and low N conditions for these NPQ kinetics traits were observed across the association panel at some but not all developmental stages (Fig. 2A). The average rate of NPQ induction and relaxation for the association panel ($NPQrate\ constant_{light}$ and $NPQrate\ constant_{dark}$) were significantly different ($P \le 0.01$, two tailed t-test) between control and low N treatments at two and three developmental stages, respectively. The speed of NPQ relaxation in the dark was significantly faster under low N treatment than control conditions ($NPQrate\ constant_{dark}$) at all three developmental stages. The effect of

low-N-treatment on the speed of NPQ induction in the light (NPQrate constant_light) was statistically significant, but not consistent across stages with a significant decrease and significant increase in early- and late-vegetative stages, respectively. Changes in NPQ steady state (NPQa-symptote_light, NPQ_max) were only statistically significant at the post-flowering stage, where both traits were significantly lower in low-N than under control conditions. At the post-flowering stage, incomplete relaxation of NPQ was more commonly observed after a 10 min dark incubation (NPQresidual_dark) under low N conditions relative to control.

In all six combinations of N-treatment and developmental stage $NPQrate\ constant_{light}\ was\ significantly\ negatively\ correlated\ with <math>NPQasymptote_{light}\ and\ NPQ_{max}\ (average\ Pearson\ correlation\ coefficient\ (r)=-0.46,\ P\leq0.001;\ Fig.\ 2B;\ S2\ and\ S3).$ However, the rate of NPQ relaxation in the dark was only weakly correlated with the range of NPQ relaxation (average $r=0.06;\ P>0.05$) except at post-flowering stage in low N ($r=0.32;\ P\leq0.001$). Several pairs of NPQ traits $-NPQrate\ constant_{light}\ \&\ NPQresidual_{dark}\ and\ NPQ_{max}\ \&\ NPQresidual_{dark}\ -showed$ increased correlation at later developmental stages, independent of N treatment. Correlation between different NPQ kinetics traits tended to be higher in control conditions than in low N conditions. At the LV stage 11 out of 15 pairwise correlations were higher in low N conditions than in control (Fig.\ 2B). At the PF stage, a similar but weaker trend was observed with 10 out of 15 pairwise correlations between traits greater in low N than in control (Fig.\ S2B).

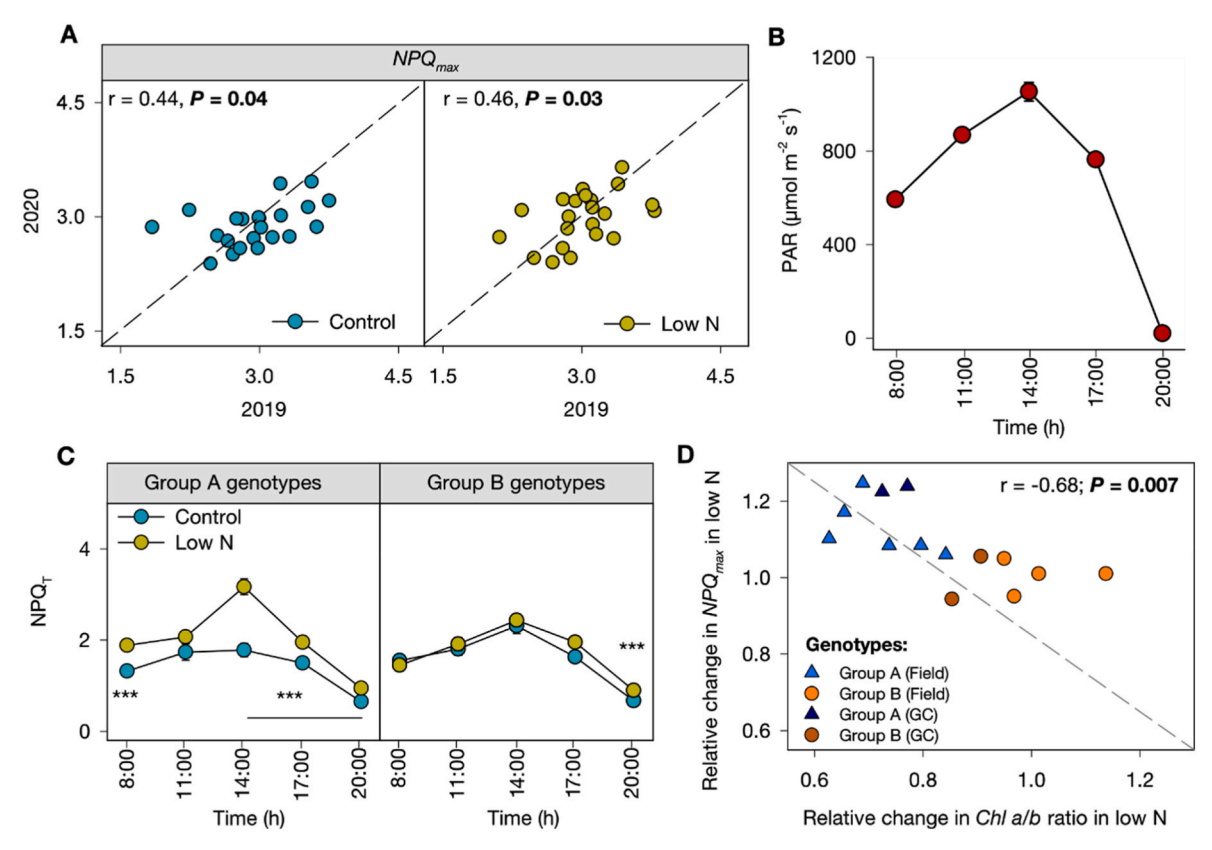


Fig. 3. NPQ consistency across years, diurnal pattern and relation to Chl a/Chl b ratio in a subset of maize ($Zea\ mays\ L$.) genotypes in two nitrogen treatments at late-vegetative stage. (A) Correlation between the maximum levels of NPQ achieved after 10 min of illumination (NPQ_{max}) for 22 maize genotypes in each of two field seasons under control and low-nitrogen conditions. Each point corresponds to one of the 22 genotypes. X-axis and y-axis indicate the best linear unbiased predictor calculated for that trait for the same genotype in 2019 and 2020, respectively. Data are the means \pm SEM (n=4 plots, each plot mean is delivered from three biological replicates). (B) Diurnal photosynthetic active radiation (PAR) on July 17, 2020. Data points are means \pm SEM of control and low-N together (n=22 genotypes) at each time point but error bars frequently are smaller than the symbol size and not visible in these cases. (C) Theoretical NPQ (NPQ $_T$) measured in Group A and Group B genotypes under control and low-N conditions in field 2020 across a diurnal time course. Genotypes Group A – genotypes with upregulated NPQ in low-N and Group B – genotypes that did not change in NPQ in low-N in either 2019 or 2020. Data points are means \pm SEM (n=11 genotypes) but frequently error bars are smaller than the symbol size. Asterisks indicate significant differences between control and low N based on two-tailed t-test (*** $P \le 0.001$). (D) Correlation between relative changes in Chl a/Chl b and NPQ_{max} under low N in 10 genotypes grown in the field in 2020 and four genotypes grown in the growth chamber. Data points are means \pm SEM (n=4 plots in field; n=4 plants in GC). In panel A and D, r and P-values correspond to Pearson's correlation coefficient and the significance of tested correlations, respectively. P- values in bold are significant ($P \le 0.005$). Data used to produce this figure are given in Dataset 2, 3 and 4.

The proportion of variance explained by genotype – as opposed to developmental stage, treatment or interaction terms – was similar for all six NPQ kinetic traits, ranging from 19 to 29% of total variance (Fig. 2C). Treatment and developmental stage explained only minimal amounts of variance in the traits analyzed. However, the effect of interaction terms between genotype (G), developmental stage (S) and treatment (T) (G \times S, G \times T, S \times T, and G \times S \times T) ranged from 0.5 to 9.3% of total variance and collectively explained a similar portion of total variance to that explained by genotype (~24%). When data from individual growth stages were analyzed independently, no one stage consistently exhibited greater broad sense heritability for NPQ kinetics traits averaging H 2 = 0.47 (values ranged from 0.30 to 0.64) (Fig. S4).

3.2. Genotypes shows consistent response of NPQ to nitrogen treatment across years and, is associated with ratios of photosynthetic pigments

A subset of 23 maize genotypes selected based to represent all three patterns of response in NPQ_{max} to low nitrogen were evaluated in a second field trial in 2020. These included 12 genotypes belonging to Group A (increased NPQ_{max} under low N), 9 genotypes belonging to Group B (no change in NPQ_{max} under low N) and 2 genotypes belonging to Group C (decrease in NPQ_{max} under low N). At the late-vegetative stage a total 800 leaf disks were collected from the 2020 field

experiment. Of these, 750 leaf disks passed quality control (QC) and were used for analysis. In addition to data QC (see the Materials and Methods section for more details), one additional leaf disk was excluded due to the lack of fluorescence signal, and a total 22 genotypes remained in the analysis. Twenty of the 22 remaining genotypes were placed into the same category, based on change in NPQ_{max} between control and low N conditions, in 2020 as they had been in 2019 (Fig. S5). The two exceptions were the genotypes - IDS91 and NC332 - placed in Group C (decrease in NPQ_{max} under low N) in 2019, but which exhibited the same range of values as Group B (no change) genotypes in 2020. The NPQmax of these 22 genotypes in both years were correlated in both in control (Pearson's correlation (r) = 0.44; P = 0.04) and low N conditions (r = 0.45; P = 0.03; Fig. 3A). Given the lack of consistent differences between Group B and Group C genotypes across multiple years, Group B and Group C genotypes are grouped together below. In order to determine whether the Group A/Group B differences were consistent throughout the day or varied diurnally, theoretical NPQ (NPQ_T) was collected from plants in the field throughout the day (Fig. 3B). Group A genotypes exhibited significantly higher NPQT over most of the day (Fig. 3C; Figs. S6 and S7). At the time point with highest light intensity (14:00 h) the NPQ_T was \sim 0.8-fold higher (P < 0.001; Fig. 3C; Fig. S8) in Group A of genotypes on low N than on control. For Group B genotypes diurnal response of NPQ_T looked almost identical in both N treatments except

Table 1
Quantification of photosynthesis-related pigments in Group A (increase NPQ in low N) and Group B (no change in NPQ in low N) genotypes under control and low nitrogen treatments in the field and growth chamber.

Group	Genotype	Chl a		Chl b		Chl a/b		Total Chl		Total Caro		Total Caro/Chl a	
		FIELD											
		Control	Low N	Control	Low N	Control	Low N	Control	Low N	Control	Low N	Control	Low N
Group A	CML333	$9.28 \pm$	6.71 ±	$2.79~\pm$	$2.69 \pm$	3.41 \pm	$2.52~\pm$	12.07 \pm	9.40 ±	2.71 \pm	2.31 ±	$0.29 \pm$	0.35
		0.33	0.42**	0.29	0.19	0.32	0.21	0.54	0.48**	0.03	0.04***	0.01	$\pm \ 0.02$
	M14	7.80 \pm	$6.79 \pm$	$2.59 \pm$	$2.79 \pm$	3.07 \pm	2.44 ±	10.38 \pm	9.58 \pm	$2.89~\pm$	$2.26 \pm$	$0.37~\pm$	0.34
		0.43	0.46***	0.27	0.19	0.21	0.08*	0.67	0.61	0.05	0.09***	0.02	$\pm~0.03$
	MO1W	8.45 \pm	6.55 ±	$2.69 \pm$	3.10 \pm	3.17 \pm	$2.18 \pm$	11.14 \pm	9.66 ±	2.77 \pm	$2.01 \pm$	$0.33 \pm$	0.31
		0.26	0.14***	0.12	0.32	0.20	0.14***	0.23	0.33*	0.11	0.16**	0.01	$\pm~0.03$
	MS153	8.97 \pm	$6.80 \pm$	$3.07 \pm$	$3.59~\pm$	$2.93 \pm$	1.92 ±	12.04 \pm	$10.39 \pm$	$2.89~\pm$	$2.18 \pm$	0.32 \pm	0.32
		0.41	0.21*	0.13	0.17	0.11	0.27*	0.51	0.06**	0.07	0.10*	0.01	$\pm~0.02$
	NC356	7.17 \pm	5.17 ±	$2.50 \pm$	$2.13~\pm$	2.91 \pm	2.45 \pm	$9.67 \pm$	7.29 \pm	$2.73 \pm$	$2.11 \pm$	$0.39 \pm$	0.41
		0.72	0.26*	0.32	0.16	0.16	0.10	1.01	0.40	0.06	0.13**	0.04	$\pm~0.02$
	Tzi8	8.20 \pm	$6.07 \pm$	2.83 \pm	3.31 \pm	2.99 \pm	1.87 ±	$11.03 \pm$	9.38 ±	3.16 \pm	$2.38 \pm$	0.38 \pm	0.39
		0.31	0.25**	0.32	0.20	0.27	0.13*	0.59	0.12*	0.26	0.13*	0.03	$\pm~0.02$
Group B	H100	9.32 \pm	7.28 ±	$3.58 \pm$	$2.91 \pm$	$2.60 \pm$	$2.52~\pm$	12.90 \pm	10.20 \pm	$3.06 \pm$	$2.56 \pm$	$0.33 \pm$	0.34
		0.20	0.79*	0.09	0.34	0.03	0.11	0.28	1.11	0.33	0.50	0.04	± 0.05
	L317	8.55 ±	7.56 ±	3.76 ±	3.41 ±	2.46 ±	2.33 ±	$12.31 \pm$	10.97 \pm	3.35 ±	2.74 ±	0.39 ±	0.36
		0.59	1.37	0.60	0.80	0.40	0.16	0.99	2.17	0.56	0.62	0.05	± 0.05
	NC312	6.73 ±	5.95 ±	$2.77~\pm$	$2.52 \pm$	2.40 ±	2.44 ±	9.50 ±	8.47 ±	$2.75 \pm$	$2.19 \pm$	0.44 ±	0.37
	110012	1.51	0.54	0.52	0.34	0.37	0.23	1.96	0.80	0.46	0.26	0.04	± 0.02
	NC332	6.62 ±	$7.21~\pm$	2.55 ±	2.49 ±	2.64 ±	3.01 ±	9.17 ±	9.70 ±	2.88 ±	2.78 ±	0.45 ±	0.39
	110002	0.55	0.38	0.30	0.21	0.23	0.45	0.79	0.25	0.16	0.16	0.05	± 0.01
P value	Treatment (T)	< 0.0001	0.00	0.90	0.21	<0.0001	0.10	0.0003	0.20	<0.0001	0.10	0.57	± 0.01
	Genotype (G)	0.009		0.01		0.21		0.006		0.41		0.03	
	$G \times T$	0.33 GROWTH	CHAMBER	0.69		0.02		0.78		0.99		0.67	
Group A	MS153	$\begin{array}{l} \textbf{6.51} \pm \\ \textbf{0.70} \end{array}$	3.78 ± 0.55*	$\begin{array}{c} \textbf{2.99} \pm \\ \textbf{0.50} \end{array}$	$\begin{array}{c} 2.22 \pm \\ 0.37 \end{array}$	$\begin{array}{c} \textbf{2.23} \pm \\ \textbf{0.12} \end{array}$	1.72 ± 0.11*	9.50 ± 1.19	6.00 ± 0.90*	$\begin{array}{c} 1.08 \pm \\ 0.19 \end{array}$	0.48 ± 0.07*	$\begin{array}{c} 0.16 \; \pm \\ 0.02 \end{array}$	$\begin{array}{c} 0.13 \\ \pm \ 0.01 \end{array}$
	Mo1W	$\begin{array}{c} \textbf{7.82} \pm \\ \textbf{0.37} \end{array}$	4.33 ± 0.66**	$\begin{array}{c} 3.32 \pm \\ 0.17 \end{array}$	2.50 ± 0.20*	$\begin{array}{c} \textbf{2.36} \pm \\ \textbf{0.03} \end{array}$	1.71 ± 0.15**	$11.14 \pm \\ 0.53$	6.82 ± 0.84**	$\begin{array}{c} \textbf{1.35} \pm \\ \textbf{0.04} \end{array}$	0.85 ± 0.16*	$\begin{array}{c} 0.17 \pm \\ 0.01 \end{array}$	$\begin{array}{c} 0.20 \\ \pm \ 0.03 \end{array}$
Group B	NC312	7.63 \pm	5.34 ±	3.27 \pm	2.32 \pm	2.32 \pm	$2.56 \pm$	10.90 \pm	7.66 ±	$1.36 \pm$	$1.01~\pm$	0.17 \pm	0.19
		0.32	0.36**	0.60	0.14	0.14	0.42	0.29	0.37***	0.34	0.11	0.04	$\pm~0.01$
	H100	$6.68 \pm$	4.60 ±	3.17 \pm	$2.39~\pm$	2.32 \pm	$1.98~\pm$	$9.85 \pm$	6.99 ±	$1.18~\pm$	0.85 \pm	0.17 \pm	0.18
		0.49	0.24**	0.59	0.18	0.39	0.22	0.48	0.08***	0.26	0.15	0.03	± 0.03
P value	Treatment (T)	< 0.0001		0.006		0.02		< 0.0001		0.003		0.87	
	Genotype (G)	0.06		0.89		0.24		0.144		0.19		0.35	
	$G \times T$	0.49		0.99		0.84		0.75		0.87		0.64	

for the last point of the diurnal cycle at 20:00 h. Group B genotypes also exhibited consistent quantum yield distribution into $\Phi_{NPQ}~(P=0.10),$ $\Phi_{PSII}~(P=0.17)$ and $\Phi_{NO}~(P=0.09)$ across N treatments (Fig. S8), while Group A genotypes exhibited a significant shift in higher $\Phi_{NPQ}~(P=0.0001)$ and lower Φ_{PSII} and $\Phi_{NO}~(P\leq0.01;$ Fig. S8).

Chlorophyll abundance was assayed in a subset of ten maize genotypes in the same field experiment. As expected, plants grown under low-nitrogen treatment accumulated less total chlorophyll than did maize genotypes grown under control conditions. This reduction was proportionally greater for chlorophyll (Chl) a (average 18%; P < 0.0001) and proportionally smaller for Chl b (average 0.6%; P = 0.9) (Table 1). However, in Group B genotypes where NPQmax did not consistently change between nitrogen treatments, the ratio of Chl a to Chl b also remained largely constant between treatments. The greater decrease in Chl a under low N was driven entirely by Group A genotypes where the average Chl a/Chl b ratio declined from 3.1 under control conditions to 2.5 under low N conditions (average 18%; $P \leq 0.05$). Consequently, the relative change in Chl a/Chl b and NPQ_{max} on low N could be described by a single highly negative correlation (r = -0.68; P= 0.007; Fig. 3D). Group A genotypes also exhibited a significant drop in total carotenoid content (average \sim 23%; $P \leq 0.04$) which was not observed in Group B genotypes ($P \ge 0.33$). Patterns of change in Chl a/Chl b ratios between treatments in the growth chamber were also consistent with the larger field study: Group A genotypes exhibited significant decreased in Chl a/Chl b ratios under low N ($P \le 0.02$) while

Group B genotypes exhibited consistent ($P \ge 0.48$) Chl a/Chl b ratios between low N and control conditions (Table 1).

3.3. Maize genotypes with elevated NPQ under low N exhibit compromised photosynthesis and reduced biomass accumulation

The responses of two pairs of genotypes representing Group A, increased NPQ under low N (MS153 and Mo1W) and Group B, no change in NPQ under low N (NC312 and H100) were also evaluated in controlled environment (e.g. growth chamber) conditions. Differences in NPQ kinetics between nitrogen treatments were largely consistent between growth chamber and field trial data at the late vegetative stage (Fig. 4A) and these same four genotypes exhibited largely consistent NPQ kinetic responses to low nitrogen in multiple years and at multiple development stages (S9 and S10). The majority of NPQ traits were higher in Group A genotypes under low N relative to control at the late vegetative stage (Fig. 4B) while Group B genotypes showed no statistically significant change in NPQ traits between treatments (\sim 0.95%; $P \ge$ 0.32). The increase in NPQ induction under low-nitrogen conditions among Group A genotypes remained statistically significant when NPQ was induced by 900 or 2000 μ mol m⁻² s⁻¹ light ($P \le 0.01$) and Group B genotypes showed no change in NPQ induction in response to low N (P \geq 0.08), however at lower (150 and 500 μ mol m⁻² s⁻¹) light intensities there were not consistent differences between groups (Figs. S11A-E).

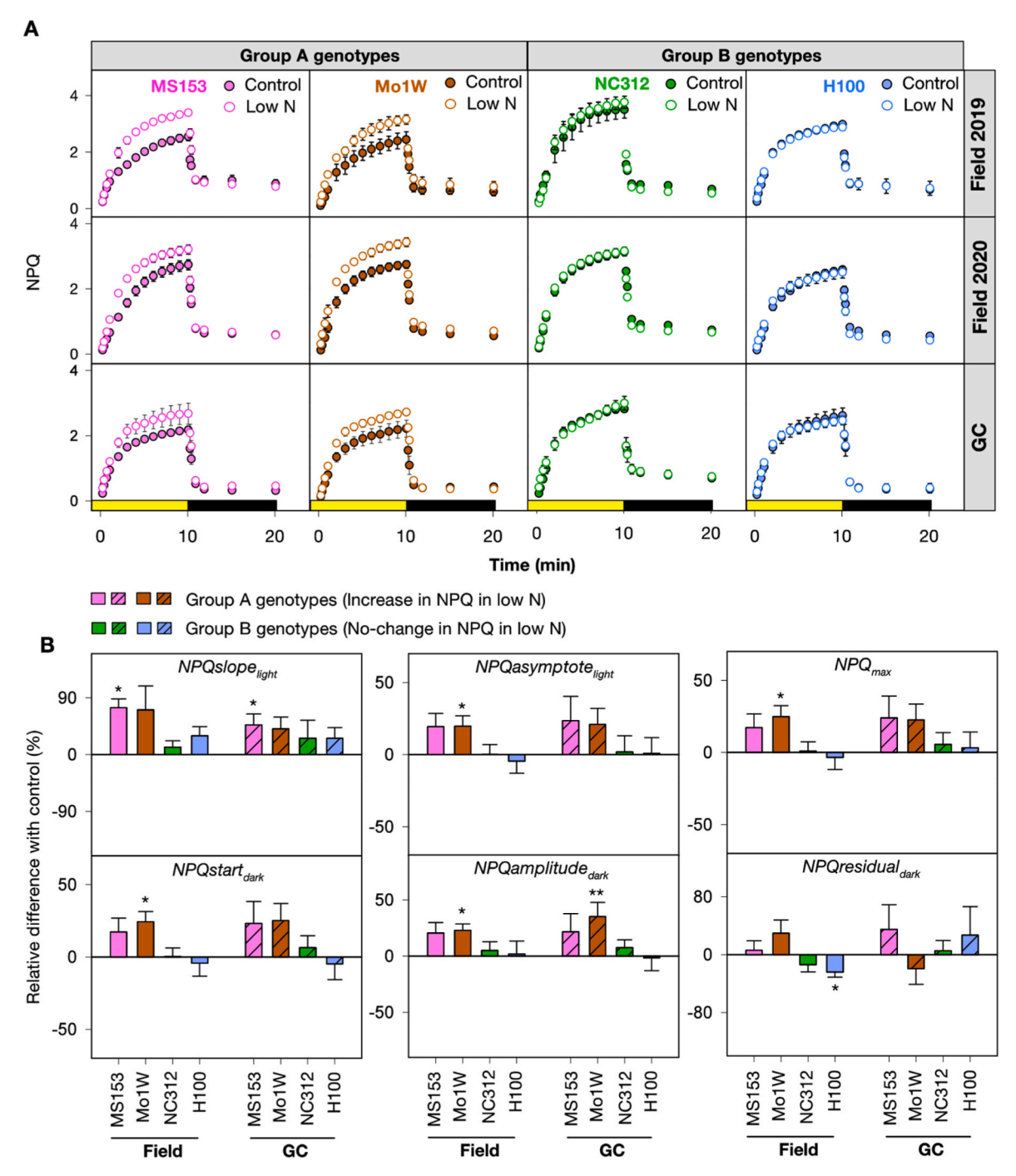


Fig. 4. Comparison of NPQ kinetic responses to nitrogen treatments across three environments in four maize ($Zea\ mays\ L$.) genotypes at the late-vegetative stage. (A) Response of NPQ induction in light (indicated in yellow horizontal bar) followed by relaxation in dark (indicated by black horizontal bar) in two groups of genotypes; MS153, Mo1W (increase NPQ in low N; Group A genotypes), and NC312 and H100 (no change in NPQ in low N; Group B genotypes) in the 2019 and 2020 field seasons and in growth chamber (GC). (B) Relative differences (%) in each NPQ trait in light ($NPQslope_{lighb}\ NPQasymptote_{lighb}\ and\ NPQ_{max}$) and dark ($NPQstart_{dark}$, $NPQamplitude_{dark}$) for each genotype under low N correspond to their control treatments in 2020 field and GC conditions. Symbols and bars are the means \pm SEM (n = 4 plots in field and n = 4 plants in GC). In panel B, asterisks indicate significant differences between control and low N based on two paired t-test (* $P \le 0.05$; * $P \le 0.01$; * $P \le 0.01$). Data used to produce this figure are given in Dataset 1, 2 and 5. (For interpretation of the references to color in this figure legend, the reader is referred to the Web version of this article.)

Group A genotypes showed an increase in proton motive force (ECS_T) under low N, similar in magnitude to the increase in NPQ_T, (\sim 56%; Figs. S12A and B). Group B genotypes also showed an increase in ECS_T under low N but the increase was smaller than that observed for Group A. All genotypes showed increases in the fraction of PSI oxidized centers (PSI_{oxc}), and decreases both in proton conductivity (gH⁺) and fraction of photosystem I active centers (PSI_{ac}) under low N relative to control,

however these changes tended to be larger in magnitude in Group A than in Group B (Fig. S12 C, D and F).

Group A genotypes had on average higher net CO_2 assimilation (A_n) , photosynthetic electron transport (J) and stomatal conductance (g_s) than Group B genotypes under control conditions (Fig. 5). However, Group A genotypes lost relatively more photosynthetic capacity particularly under low N at high light intensities. For instance, A_{sat} decreased by 75%

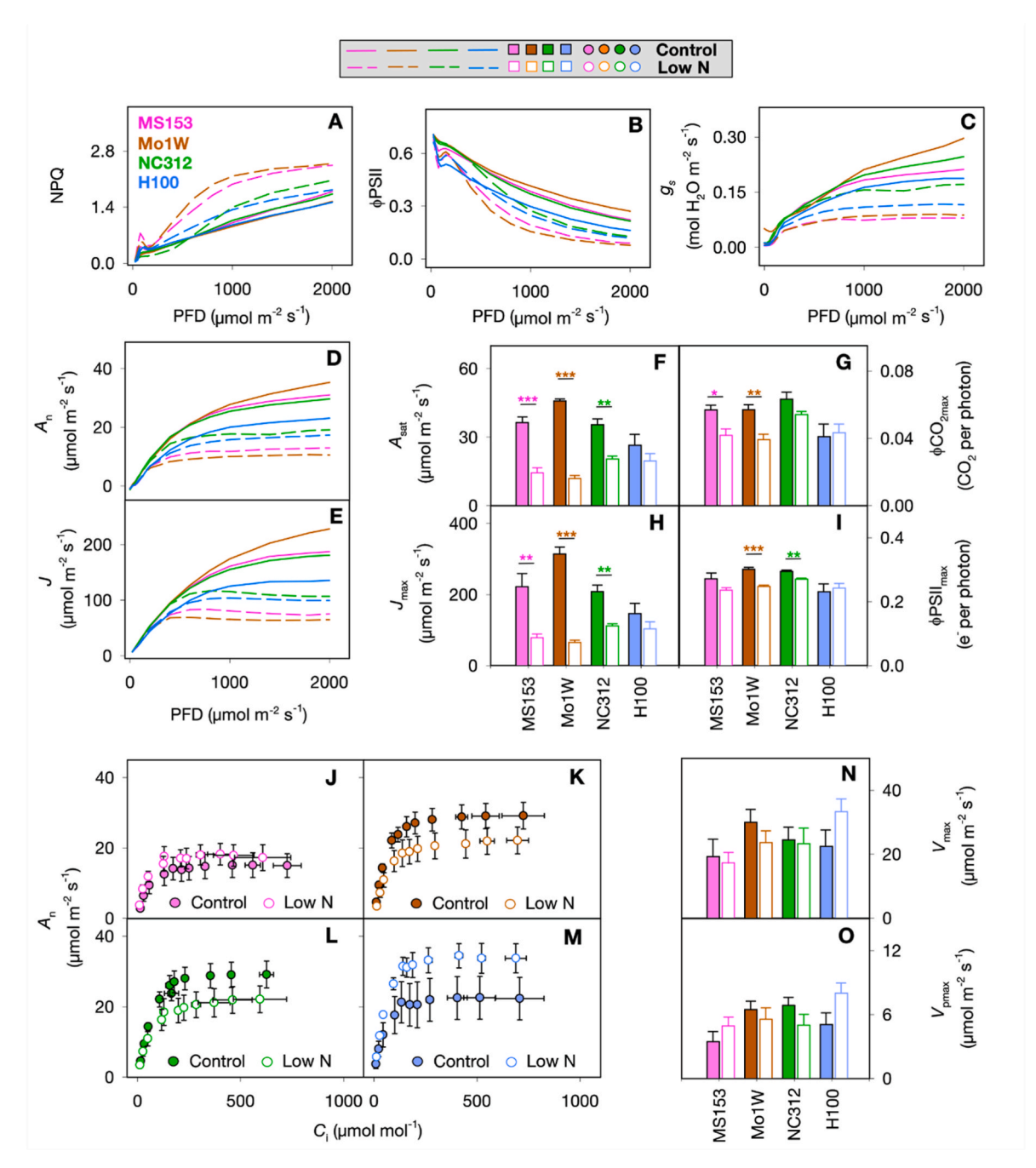


Fig. 5. Response of gas-exchange and fluorescence-related photosynthesis parameters to steady-state changes in light and intercellular CO_2 concentration (C_i) in four maize (*Zea mays* L.) genotypes grown under two nitrogen treatments under growth-chamber conditions. (A) NPQ, (B) photosystem II operating efficiency ($\Phi PSII$), (C) stomatal conductance (g_s), (D) net CO_2 fixation rate (A_n), and (E) linear electron transport rate (J) as a function of step increases in incident photon flux density (PFD). (F) Quantum efficiency of leaf net CO_2 assimilation (ΦCO_{2max}), (G) light-saturated rate of net CO_2 assimilation rate (A_{sat}), (H) maximal linear electron transport rate (J_{max}), and (I) quantum efficiency of linear electron transport ($\Phi PSII_{max}$). (J–M) A_n measured as a function of gradual changes in C_i . (N) Maximal velocity of Rubisco for carboxylation (V_{pmax}), and (O) [CO_2]-saturated velocity of A_n (V_{max}). All traits were measured in the late-vegetative stage in MS153, Mo1W (increase NPQ in low N; Group A genotypes), and NC312 and H100 (no-change in NPQ in low N; Group B genotypes) under control (solid line, bar and circle) and low N (dashed line, open bar or open circle) treatments. Data are the means \pm SEM (n = 4 biological replicates). Asterisks show significant differences in low N from the control (paired t-test; *P \leq 0.00; **P \leq 0.01; ***P \leq 0.001). Data used to produce this figure are given in Dataset 6 and 7.

 $(P \leq 0.0005)$ in both MS153 and Mo1W. However, in NC312 and H100, the same trait decreased but only by 25% (P=0.002) and 10% (P=0.28), respectively (Fig. 5F). Genotypes showed very similar differences in $J_{\rm max}$ to these observed for $A_{\rm sat}$ (Fig. 5H). In the light-limited portion of the A_n /light-response (Q) and J/Q curves the difference between treatments and genotypes were less pronounced. Nevertheless, quantum efficiency of leaf net CO_2 assimilation (ΦCO_{2max}) decreased by an average of 29% $(P \leq 0.02)$ in Group A genotypes and only a statistically

insignificant 14% ($P \le 0.8$) in Group B genotypes (Fig. 5G). PSII operating efficiency ($\Phi PSII_{max}$) followed a similar trend to that observed for ΦCO_{2max} (Fig. 5I). The preceding results were measured under constant light, however results under fluctuating light were largely consistent with those under constant light (Fig. S13) with the exception of the g_s/Q curves (Fig. S13C) where stomatal response to low light was reduced under low N relative to control. CO_2 response curves (A/C_i curves) showed substantial variation among genotypes in the maximal rate of

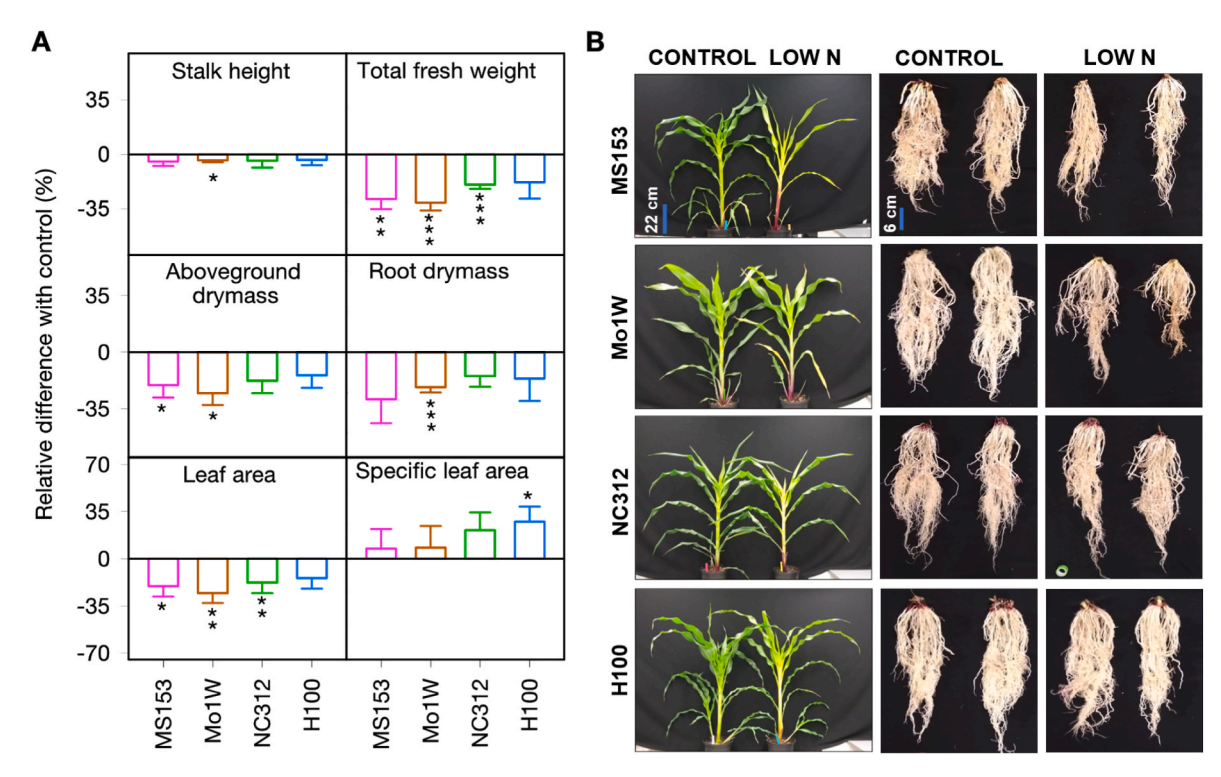


Fig. 6. Morphological responses of four maize (*Zea mays* L.) genotypes to control and low-nitrogen treatments. (A) Stalk height, total fresh weight, above-ground drymass, root dry mass, leaf area and specific leaf area under low N expressed as relative difference with the same traits measured from the same genotypes under control conditions (%). (B) Illustration of changes in above- and below-ground plant organs between treatments. All traits were measured in the late-vegetative stage for all four genotypes (MS153, Mo1W (Group A)), and NC312 and H100 (Group B) under control and low-nitrogen treatments. Above-ground scale bar = 22 cm and below-ground scale bar = 6 cm. Data are the means \pm SEM (n = 4 biological replicates). Asterisks indicate significant differences between low nitrogen and control (paired *t*-test; * $P \le 0.05$; ** $P \le 0.01$; *** $P \le 0.01$; *** $P \le 0.01$. Data used to produce this figure are given in Dataset 8.

phosphoenolpyruvate (PEP) carboxylation (V_{pmax}) and [CO₂]-saturated rate of A (V_{max}) determined by capacity for PEP regeneration and leakage of CO₂ from the bundle sheath were not significantly different (P > 0.05) between treatments for any of the four analyzed genotypes (Fig. 5G-O).

The changes in NPQ kinetics, photosynthetic pigment ratios, and photosynthetic traits between Group A and Group B genotypes under low N were associated with different biomass accumulation outcomes. All four genotypes showed substantial decrease in plant size on low N relative to control conditions, however, the decreases in biomass were proportionally greater for Group A genotypes than Group B genotypes (Fig. 6). Low N treatment resulting in a reduction in total fresh weight, above ground dry biomass, and root dry mass of $\sim\!35\%$ each among the two Group A genotypes ($P \le 0.004$, $P \le 0.04$, and P = 0.0005) (Fig. 6A) as well as a reduction in leaf area of $\sim\!25\%$ ($P \le 0.03$). The same traits in Group B genotypes were reduced by $\sim\!15\%$ with only total fresh weight and leaf area being significantly lower in one out of two analyzed genotypes (NC312; P < 0.007).

4. Discussion

An understanding of how plants respond to the rapid changes in light intensity experienced in many natural and agricultural settings has driven interest over multiple decades in investigating the photosynthetic processes including NPQ (Demmig-Adams and Adams, 1992; Murchie and Niyogi, 2011; Kaiser et al., 2018; Wang et al., 2020). NPQ is a core component of photosynthesis and plant fitness (Külheim et al., 2002). A growing body of evidence supports the existence of substantial variation in the maximum inducible NPQ values which can be obtained by different genotypes of the same species ranging from arabidopsis (Rungrat et al., 2019) to rice (Jung and Niyogi, 2009; Wang et al., 2017; Rungrat et al., 2019) and soybean (Burgess et al., 2020). In the diverse

panel of 225 maize genotypes we evaluated here, the difference in NPQ_{max} between the genotypes most and least responsive to high light treatment was >2x in each combination of nitrogen treatment and developmental stage (Fig. 1A). This degree of phenotypic diversity was approximately double the range reported for the same trait in surveys of diverse arabidopsis (Rungrat et al., 2019) and soybean (Burgess et al., 2020) populations. In the low-nitrogen treatment at the post-flowering stage of development, the stage at which the effects of low-nitrogen stress became most extreme, this range expanded even further to a 5x difference between the genotypes most and least responsive to high light treatment. Our results are consistent with Rungrat et al. (2019) and suggest that variation in NPQ is dependent on the growth stage at which they were measured and underline the importance of considering the plant developmental stage in NPQ studies particularly under abiotic stresses.

The extension of the study of NPQ kinetics from the use of single model genotypes to populations has enabled the identification of both substantial genetically-controlled diversity, and specific genetic loci controlling variation in NPQ kinetic traits (Wang et al., 2017; Rungrat et al., 2019; Sahay et al., 2023). However, optimal NPQ kinetic responses to maximize photosynthetic productivity likely vary across environments. In our initial study, we were able to identify sets of maize genotypes where NPQ_{max} increased, decreased, or remained unchanged under low N treatment relative to control conditions (Fig. 1B). Of these three potential patterns, genotypes exhibiting two potential responses (increased NPQ_{max} under low N and no change in NPQ_{max} under low N) continued to exhibit consistent responses across multiple years, throughout the day (diurnally), higher light intensities as well as between field and controlled environment conditions (Fig. 3A–C; Fig. 4; Figs. S11B–D), indicating the inherent genetic variation in NPQ.

Quantum yields of photochemistry, NPQ, and other unregulated dissipation processes were also measured by parameters Φ_{PSII} , Φ_{NPO} , and

 Φ_{NO} , respectively in two groups (A and B) of genotypes under low N stress condition (Figs. S7 and S8). A large increase in Φ_{NPQ} induced a significant decrease in Φ_{PSII} in genotypes where NPQ increased under low N (group A) suggest that a photosynthetic yield was determined largely by a greater NPQ-dependent energy dissipation, and less energy by other unregulated dissipation (Fig. S8). The result indicates that, under low N stress, these plants favored the light-dependent dissipative processes (Φ_{NPQ}, NPQ_T) over other mechanisms (Kasajima et al., 2011; Gómez et al., 2018).

Higher ECS_T (estimates proton motive force) and decreased gH⁺ (estimates ATPase synthase activity) in thylakoid membrane in genotypes where NPQ increased in response to nitrogen deficit, implying an effect on light-driven proton transfer to increase ΔpH and may reflect the activation of qE (Fig. S12) via activation violaxanthin deepoxidation and protonation of the photosystem II subunit S protein (Li et al., 2000; Kanazawa and Kramer, 2002; Rott et al., 2011; Kanazawa et al., 2017; Takagi et al., 2017). Similar dependence of NPQ induction on the downregulation of chloroplastic ATP synthesis was observed in cold-treated tobacco (Yang et al., 2018). Our results support the conclusion that higher qE induction (as indicated by the NPQ_{max} and NPO_T) was caused by higher amplitude of light-induced thylakoid pmf (ECS_T) changes in low N stressed plants. Low N stress, in both group A and B genotypes, led to increase in steady state P700⁺ oxidation state (PSI_{oxc}) and no change in reduction state (PSI_{orc}) indicating that electron flow from PSII to PSI was likely limited at cytochrome b6f complex (so-called Photosynthesis Control), which is linked to the low lumen pH (Colombo et al., 2016; Kanazawa et al., 2017).

While total chlorophyll (except NC332) and carotenoid content declined in all maize genotypes tested under low-nitrogen conditions, significant decreases in Chl a/Chl b ratios due to increase in Chl b relative to Chl a) were observed only in the set of maize genotypes in which NPQmax increased significantly under low-nitrogen treatment relative to controls (Table 1). This result is consistent with a previous report that an increase in NPQ_{max} was associated with a decrease in Chl a/Chl b ratios in a chinese maize hybrid when grown under low N (Lu and Zhang, 2000). Similar observations have also been reported for cassava (Manihot esculenta) grown on low N (Cruz et al., 2003). Interestingly, in other stress related to nutrients availability (salt stress) in sorghum (Sorghum bicolor; Netondo et al., 2004) and beach plum (Prunus maritima; Zai et al., 2012) preserved similar Chl a/Chl b to that in control what correlated with unchanged NPQ. Study of A. thaliana chlorophyll b-less mutants showed that light-harvesting chlorophyll a/b-protein complexes play multiple roles in defining structure and optimal function of chloroplasts (Kim et al., 2009). For instance, in the chlorophyll b-less mutants the content of all six light harvesting proteins of PSII was greatly diminished that led to the surface of thylakoids less negatively charged and increased light-independent thermal dissipation in PSII compared to that wild type. Bru et al. (2020) showed that pale green, high NPQ and normal $F_{\nu}/F_m A$. thaliana mutant class has lower Chl a/Chl b and speculated that this phenotype might be due to a mutation in a gene coding for a light-harvesting chlorophyll a/b-binding proteins or a factor involved in their transcriptional regulation.

The significant relative decrease in chlorophyll a suggests a greater loss in reaction center complexes and reengineering of the photosynthetic apparatus among maize genotypes where NPQ_{max} increases under low N treatment. In other words, fewer PSII reaction centers with larger PSII antenna led to a more shade like phenotype in group A genotype. Therefore, relatively more excitation energy could be funneled to fewer PSII reaction centers in the responsive maize genotypes than the unresponsive ones. This increase in excitation energy per reaction center under low N may explain why NPQ is induced to higher levels in these genotypes relative to maize genotypes which preserve similar ratios of Chl a/Chl b across both treatments.

Our results demonstrate a modification of PSII antenna size in low N leaves, although low N had no effect on F_{ν}/F_{m} in pre-flowering (growth chamber) and late vegetative stage (field) (Fig. S14). Such a

modification reflected in a decrease in carbon assimilation (A_{sat}), more in genotypes where NPQ increased in response to low N conditions than in genotypes where NPQ remained unchanged which may explain the decreases in stomatal conductance (g_s) which were also observed in these genotypes suggesting that reduced carbon assimilation was not the result of photoinhibition (Fig. S14). While modest reductions in PEP carboxylation rate and Rubisco regeneration capacity were observed in all four genotypes, these changes were not statistically significant and insufficient to explain the reduction in overall carbon assimilation. Instead, the decrease in carbon assimilation appears to be directly linked to the observed changes in NPQ and Chl a/Chl b ratios. In genotypes where NPQmax is higher under low-nitrogen treatment than control treatment a smaller proportion of light energy captured by photosystem II ($\Phi PSII$) and electron transport (J_{max}) is reduced relative to nonresponsive genotypes. These observations, like the change in Chl a/ Chl b ratios, would be consistent with a greater decrease in photosynthetic reaction centers in genotypes where low-nitrogen stress alters NPQ kinetics. As might be expected, these changes in photosynthetic activity were associated with substantially bigger declines in fresh and dry biomass for responsive maize genotypes under low N relative to control conditions (Fig. 6), although these results should be interpreted with caution given the relatively small numbers of responsive and nonresponsive genotypes evaluated.

NPQ kinetics have long been known to change in response to the broadly defined environmental factors (Havaux and Kloppstech, 2001; Fernández-Marín et al., 2021; Nosalewicz et al., 2022; Rodrigues de Queiroz et al., 2023). More recently the kinetics of NPQ have also been shown to vary as a result of naturally occurring genetic diversity in a range of crop and wild species (Wang et al., 2017; Rungrat et al., 2019; Burgess et al., 2020; Sahay et al., 2023). Differences were observed in how NPQ responded to drought between two sorghum genotypes with differing drought stress tolerance (Baker et al., 2023). Here, we have demonstrated that variation in NPQ kinetics resulted from genetic and environmental factors, are not independent of each other. Instead, different genotypes exhibit differential plasticity of NPQ response to the same environmental perturbations. These genetically-controlled differences in how environmental changes alter NPQ kinetics are, in turn, associated with differences in both the photosynthetic apparatus and photosynthetic productivity, as well as differences in overall biomass accumulation. Since thermal dissipation of excess excitation energy measured via NPQ helps to balance the energy absorbed with energy utilized, the NPO changes are the reflection of molecular and biochemical changes which occur under low N. In our study, the genotype-dependent responses observed under low N might be due to differential expression of genes related to chlorophyll catabolism like stay-green gene (Baker et al., 2023), light-harvesting chlorophyll a/b-binding genes (Bru et al., 2020) as well as gene involved broadly in N assimilation.

Natural genetic variation controlling plastic responses of NPQ kinetics to environmental perturbation increases the likelihood it will be possible to optimize NPQ kinetics in crop plants for different environments. Our results also suggest that screening for genotypes which exhibit large increases in NPQ_{max} or proxy traits in different environments may serve as a comparatively low cost and high-throughput method to identify crop genotypes where photosynthetic health and productivity is compromised in different environments or in response to different stresses, particularly as we were able to recapitulate the differences between responsive and nonresponsive genotypes initially observed from leaf disk assays with in-field estimates of NPQ (e.g. NPQ_T).

CRediT authorship contribution statement

Seema Sahay: Writing – review & editing, Writing – original draft, Visualization, Methodology, Investigation, Formal analysis, Data curation. **Marcin Grzybowski:** Writing – review & editing, Visualization,

Methodology, Investigation, Data curation. **James C. Schnable:** Writing – review & editing, Visualization, Supervision, Funding acquisition, Conceptualization. **Katarzyna Głowacka:** Writing – review & editing, Writing – original draft, Visualization, Supervision, Methodology, Funding acquisition, Conceptualization.

Declaration of competing interest

The authors declare that they have no known competing financial interests or personal relationships that could have appeared to influence the work reported in this paper.

Data availability

Data are being made available in supplemental datasets associated with this paper.

Acknowledgements and Funding

We would like to acknowledge Brandi Sigmon and Christine Smith for designing and executing the field experiments in 2019 and 2020. The authors thank Annie Nelson, Himani Patel and Marie Barnald for assistance in the collection of leaf disks from the field and imaging them in the lab. We also thank the anonymous reviewers for their insightful comments and constructive suggestions in improving the quality of our manuscript during the revision process. This research was supported by the National Science Foundation under award no. OIA-1557417 for the Center for Root and Rhizobiome Innovation (CRRI). KG was supported by the National Science Foundation supporting Nebraska Established Program to Stimulate Competitive Research program under FIRST Award, Layman Fund held at the University of Nebraska Foundation and National Science Foundation CAREER grant no. 2142993.

Appendix A. Supplementary data

Supplementary data to this article can be found online at https://doi.org/10.1016/j.jplph.2024.154261.

References

- Baker, C.R., Patel-Tupper, D., Cole, B.J., Ching, L.G., Dautermann, O., Kelikian, A.C., Allison, C., Pedraza, J., Sievert, J., Bilbao, A., Lee, J.Y., Kim, Y.M., Kyle, J.E., Bloodsworth, K.J., Paurus, V., Hixson, K.K., Hutmacher, R., Dahlberg, J., Lemaux, P. G., Niyogi, K.K., 2023. Metabolomic, photoprotective, and photosynthetic acclimatory responses to post-flowering drought in sorghum. Plant Direct 7, e545.
- acclimatory responses to post- flowering drought in sorghum. Plant Direct 7, e545.Baggs, E.M., Rees, R.M., Smith, K.A., Vinten, A.J.A., 2006. Nitrous oxide emission from soils after incorporating crop residues. Soil Use Manag. 16, 82–87.
- Bi, Y.-M., Kant, S., Clarke, J., Gidda, S., Ming, F., Xu, J., Rochon, A., Shelp, B.J., Hao, L., Zhao, R., Mullen, R.T., Zhu, T., Rothstein, S.T., 2009. Increased nitrogen-use efficiency in transgenic rice plants over-expressing a nitrogen-responsive early nodulin gene identified from rice expression profiling. Plant Cell Environ. 32, 1749–1760.
- Bilger, W., Björkman, O., 1994. Relationships among violaxanthin deepoxidation, thylakoid membrane conformation, and nonphotochemical chlorophyll fluorescence quenching in leaves of cotton (Gossypium hirsutum L.). Planta 193, 238–246.
- Bru, P., Nanda, S., Malnoe, A.A., 2020. Genetic screen to identify new molecular players involved in photoprotection qH in Arabidopsis thaliana. Plants 9, 1565.
- Burgess, S.J., de Becker, E., Cullum, S., Causon, I., Floristeanu, I., Chan, K.X., Moore, C. E., Diers, B.W., Long, S.P., 2020. Variation in relaxation of non-photochemical quenching in a soybean nested association mapping panel as a potential source for breeding improved photosynthesis. bioRxiv 2020, 201210, 07.29.
- Burgess, A.J., Retkute, R., Preston, S.P., Jensen, O.E., Pound, M.P., Pridmore, T.P., Murchie, E.H., 2016. The 4-dimensional plant: effects of wind-induced canopy movement on light fluctuations and photosynthesis. Front. Plant Sci. 7, 1392.
- Caemmerer von, S., 2000. Biochemical Models of Leaf Photosynthesis. CSIRO Publishing. Melbourne, VIC, Australia.
- Cao, P., Lu, C., Yu, Z., 2018. Historical nitrogen fertilizer use in agricultural ecosystems of the contiguous United States during 1850–2015: application rate, timing, and fertilizer types. Earth Syst. Sci. Data 10, 969–984.
- Ciampitti, I.A., Briat, J.-F., Gastal, F., Lemaire, G., 2022. Redefining crop breeding strategy for effective use of nitrogen in cropping systems. Commun. Biol. 5, 823.
- Colombo, M., Suorsa, M., Rossi, F., Ferrari, R., Tadini, L., Barbato, R., Pesaresi, P., 2016. Photosynthesis control: an underrated short-term regulatory mechanism essential for plant viability. Plant Signal. Behav. 11, e1165382.

- Cruz, J.L., Mosquim, P.R., Pelacani, C.R., Araújo, W.L., DaMatta, F.M., 2003. Photosynthesis impairment in cassava leaves in response to nitrogen deficiency. Plant Soil 257, 417–423.
- Demmig-Adams, B., Adams, W.W., 1992. Photoprotection and other responses of plants to high light stress. Annu. Rev. Plant Physiol. Plant Mol. Biol. 43, 599–626.
- De Souza, A.P., Burgess, S.J., Doran, L., Hansen, J., Manukyan, L., Maryn, N., Gotarkar, D., Leonelli, L., Niyogi, K.K., Long, S.P., 2022. Soybean photosynthesis and crop yield are improved by accelerating recovery from photoprotection. Science 377, 851–854.
- Diaz, C., Saliba-Colombani, V., Loudet, O., Belluomo, P., Moreau, L., Daniel-Vedele, F., Morot-Gaudry, J.-F., Masclaux-Daubresse, C., 2006. Leaf yellowing and anthocyanin accumulation are two genetically independent strategies in response to nitrogen limitation in Arabidopsis thaliana. Plant Cell Physiol. 47, 74–83.
- Ding, L., Wang, K.J., Jiang, G.M., Biswas, D.K., Xu, H., Li, L.F., Li, Y.H., 2005. Effects of nitrogen deficiency on photosynthetic traits of maize hybrids released in different years. Ann. Bot. 96, 925–930.
- Duvick, D.N., 2005. The contribution of breeding to yield advances in maize (Zea mays L.). Adv. Agron. 86, 83–145.
- FAO, 2019. Agriculture and climate change Challenges and opportunities at the global and local Level. Collaboration on Climate-Smart Agriculture. Rome.
- Fernández-Marín, B., Roach, T., Verhoeven, A., García-Plazaola, J.I., 2021. Shedding light on the dark side of xanthophyll cycles. New Phytol. 230, 1336–1344.
- Flint-Garcia, S.A., Thuillet, A.-C., Yu, J., Pressoir, G., Romero, S.M., Mitchell, S.E., Doebley, J., Kresovich, S., Goodman, M.M., Buckler, E.S., 2005. Maize association population: a high-resolution platform for quantitative trait locus dissection. Plant J. 44, 1054–1064.
- Garcia-Molina, A., Leister, D., 2020. Accelerated relaxation of photoprotection impairs biomass accumulation in Arabidopsis. Nat. Plants 6, 9–12.
- Garnier, E., Shipley, B., Roumet, C., Laurent, G., 2001. A standardized protocol for the determination of specific leaf area and leaf dry matter content. Funct. Ecol. 15, 688–695.
- Giles, J., 2005. Nitrogen study fertilizes fears of pollution. Nature 433, 791.
- Gómez, R., Carrillo, N., Morelli, M.P., Tula, S., Shahinnia, F., Hajirezaei, M.R., Lodeyro, A.F., 2018. Faster photosynthetic induction in tobacco by expressing cyanobacterial favodiiron proteins in chloroplasts. Photosynthetic Research 136, 129–138
- Havaux, M., Kloppstech, K., 2001. The protective functions of carotenoid and flavonoid pigments against excess visible radiation at chilling temperature investigated in Arabidopsis npq and tt mutants. Planta 213, 953–966.
- Hirel, B., Le Gouis, J., Ney, B., Gallais, A., 2007. The challenge of improving nitrogen use efficiency in crop plants: towards a more central role for genetic variability and quantitative genetics within integrated approaches. J. Exp. Bot. 58, 2369–2387.
- Jin, X., Yang, G., Tan, C., Zhao, C., 2015. Effects of nitrogen stress on the photosynthetic CO2 assimilation, chlorophyll fluorescence, and sugar-nitrogen ratio in corn. Sci. Rep. 5, 9311.
- Jung, H.-S., Niyogi, K.K., 2009. Quantitative genetic analysis of thermal dissipation in Arabidopsis. Plant Physiology 150, 977–986.
- Kaiser, E., Morales, A., Harbinson, J., 2018. Fluctuating light takes crop photosynthesis on a rollercoaster ride. Plant Physiology 176, 977–989.
- Kanazawa, A., Kramer, D.M., 2002. In vivo modulation of nonphotochemical exciton quenching (NPQ) by regulation of the chloroplast ATP synthase. Proceedings of the National Academy of Sciences of the United States of America 99, 12789–12794.
- Kanazawa, A., Ostendorf, E., Kohzuma, K., Hoh, D., Strand, D.D., Sato-Cruz, M., Savage, L., Cruz, J.A., Fisher, N., Froehlich, J.E., Kramer, D.M., 2017. Chloroplast ATP synthase modulation of the thylakoid proton motive force: Implications for photosystem I and photosystem II photoprotection. Front. Plant Sci. 8, 719.
- Kant, S., Bi, Y.-M., Weretilnyk, E., Barak, S., Rothstein, S.J., 2008. The Arabidopsis halophytic relative Thellungiella halophila tolerates nitrogen-limiting conditions by maintaining growth, nitrogen uptake, and assimilation. Plant Physiology 147, 1168–1180.
- Kasajima, I., Ebana, K., Yamamoto, T., Takahara, K., Yano, M., Kawai Yamada, M., Uchimiya, H., 2011. Molecular distinction in genetic regulation of nonphotochemical quenching in rice. Proceedings of the National Academy of Sciences of the United States of America 108, 13835–13840.
- Kitajima, M., Butler, W.L., 1975. Quenching of chlorophyll fluorescence and primary photochemistry in chloroplasts by dibromothymoquinone. Biochim. Biophys. Acta Bioenerg. 376, 105–115.
- Kim, E., Li, X., Razeghifard, M., Anderson, J.M., Niyogi, K.K., 2009. The multiple roles of light-harvesting chlorophyll a/b-protein complexes define structure and optimize function of Arabidopsis chloroplasts: a study using two chlorophyll b-less mutants. Biochim. Biophys. Acta 1787, 973–984.
- Klughammer, C., Schreiber, U., 1994. An improved method, using saturating light pulses, for the determination of photosystem I quantum yield via P700+ absorbance changes at 830 nm. Planta 192, 261–268.
- Kromdijk, J., Głowacka, K., Leonelli, L., Gabilly, S.T., Iwai, M., Niyogi, K.K., Long, S.P., 2016. Improving photosynthesis and crop productivity by accelerating recovery from photoprotection. Science 354, 857–861.
- Külheim, C., Agren, J., Jansson, S., 2002. Rapid regulation of light harvesting and plant fitness in the field. Science 297, 91–93.
- Kuhlgert, S., Austic, G., Zegarac, R., Osei-Bonsu, I., Hoh, D., Chilvers, M.I., Roth, M.G., Bi, K., TerAvest, D., Weebadde, P., Kramer, D.M., 2016. MultispeQ Beta: a tool for large-scale plant phenotyping connected to the open PhotosynQ network. R. Soc. Open Sci. 3, 160592.
- Lehretz, G.G., Schneider, A., Leister, D., Sonnewald, U., 2022. High non-photochemical quenching of VPZ transgenic potato plants limits CO2 assimilation under high light

- conditions and reduces tuber yield under fluctuating light. Journal of Integrated Plant Biology $64,\,1821-1832.$
- Li, X.P., Björkman, O., Shih, C., Grossman, A.R., Rosenquist, M., Jansson, S., Niyogi, K.K., 2000. A pigment-binding protein essential for regulation of photosynthetic light harvesting. Nature 403, 391–395.
- Lichtenthaler, H.K., 1987. Chlorophylls and carotenoids: pigments of photosynthetic biomembranes. Methods Enzymol. 148, 350–382.
- Liu, Z., Gao, J., Gao, F., Liu, P., Zhao, B., Zhang, J., 2018a. Photosynthetic characteristics and chloroplast ultrastructure of summer maize response to different nitrogen supplies. Front. Plant Sci. 9, 576.
- Liu, T., Ren, T., White, P.J., Cong, R., Lu, J., 2018b. Storage nitrogen co-ordinates leaf expansion and photosynthetic capacity in winter oilseed rape. J. Exp. Bot. 69, 2995–3007.
- Loriaux, S.D., Avenson, T.J., Welles, J.M., McDermitt, D.K., Eckles, R.D., Riensche, B., Genty, B., 2013. Closing in on maximum yield of chlorophyll fluorescence using a single multiphase flash of sub-saturating intensity. Plant Cell Environ. 36, 1755–1770.
- Lu, C., Zhang, J., 2000. Photosynthetic CO2 assimilation, chlorophyll fluorescence and photoinhibition as affected by nitrogen deficiency in maize plants. Plant Sci.: An International Journal of Experimental Plant Biology 151, 135–143.
- Maas, S.J., Dunlap, J.R., 1989. Reflectance, transmittance, and absorptance of light by normal, etiolated, and albino corn Leaves. Agron. J. 81, 105–110.
- Martin, T., Oswald, O., Graham, I.A., 2002. Arabidopsis seedling growth, storage lipid mobilization, and photosynthetic gene expression are regulated by carbon:nitrogen availability. Plant Physiology 128, 472–481.
- Meier, M.A., Xu, G., Lopez-Guerrero, M.G., et al., 2022. Association analyses of host genetics, root-colonizing microbes, and plant phenotypes under different nitrogen conditions in maize. Elife 11.
- Monneveux, P., Cabon, G., Sánchez, C., 2006. Low nitrogen tolerance in tropical quality protein maize (Zea mays L.): value of predictive traits. Cereal Res. Commun. 34, 1239–1246.
- Müller, P., Li, X.P., Niyogi, K.K., 2001. Non-photochemical quenching. A response to excess light energy. Plant Physiology 125, 1558–1566.
- Murchie, E.H., Niyogi, K.K., 2011. Manipulation of photoprotection to improve plant photosynthesis. Plant Physiology 155, 86–92.
- Netondo, G.W., Onyango, J.C., Beck, E., 2004. Sorghum and salinity. Crop Sci. 44, 806–811.
- Nilkens, M., Kress, E., Lambrev, P., Miloslavina, Y., Müller, M., Holzwarth, A.R., Jahns, P., 2010. Identification of a slowly inducible zeaxanthin-dependent component of non-photochemical quenching of chlorophyll fluorescence generated under steady-state conditions in Arabidopsis. Biochim. Biophys. Acta 1797, 466–475.
- Nosalewicz, A., Okoń, K., Skorupka, M., 2022. Non-photochemical quenching under drought and fluctuating light. Int. J. Mol. Sci. 23, 5182.
- Park, S., Croteau, P., Boering, K.A., Etheridge, D.M., Ferretti, D., Fraser, P.J., Kim, K.R., Krummel, P.B., Langenfelds, R.L., van Ommen, T.D., Steele, L.P., Trudinger, C.M., 2012. Trends and seasonal cycles in the isotopic composition of nitrous oxide since 1940. Nat. Geosci. 5, 261–265.
- Pearcy, R.W., 1990. Sunflecks and photosynthesis in plant canopies. Annu. Rev. Plant Physiol. Plant Mol. Biol. 41, 421–453.
- Peng, M., Bi, Y.-M., Zhu, T., Rothstein, S.J., 2007. Genome-wide analysis of Arabidopsis responsive transcriptome to nitrogen limitation and its regulation by the ubiquitin ligase gene NLA. Plant Mol. Biol. 65, 775–797.
- Rodene, E., Xu, G., Palali Delen, S., Zhao, X., Smith, C., Ge, Y., Schnable, J., Yang, J., 2022. A UAV-based high-throughput phenotyping approach to assess time-series nitrogen responses and identify trait-associated genetic components in maize. The Plant Phenome Journal 5, e20030.
- Rodrigues de Queiroz, A., Hines, C., Brown, J., Sahay, S., Vijayan, J., Stone, J.M., Bickford, N., Wuellner, M., Glowacka, K., Buan, N.R., Roston, R.L., 2023. The effects of exogenously applied antioxidants on plant growth and resilience. Phytochemistry Rev. 22, 407–447.

- Rodríguez-Espinosa, T., Papamichael, I., Voukkali, I., Gimeno, A.P., Candel, M.B.A., Navarro-Pedreño, J., Zorpas, A.A., Lucas, I.G., 2023. Nitrogen management in farming systems under the use of agricultural wastes and circular economy. Sci. Total Environ. 876, 162666.
- Rott, M., Martins, N.F., Thiele, W., Lein, W., Bock, R., Kramer, D.M., Schöttler, M.A., 2011. ATP synthase repression in tobacco restricts photosynthetic electron transport, CO2 assimilation, and plant growth by overacidification of the thylakoid lumen. Plant Cell 23, 304–321.
- Rungrat, T., Almonte, A.A., Cheng, R., Gollan, P.J., Stuart, T., Aro, E.-M., Borevitz, J.O., Pogson, B., Wilson, P.B., 2019. A genome-wide association study of non-photochemical quenching in response to local seasonal climates in Arabidopsis thaliana. Plant Direct 3, e00138.
- Sacksteder, C.A., Kanazawa, A., Jacoby, M.E., Kramer, D.M., 2000. The proton to electron stoichiometry of steady-state photosynthesis in living plants: a protonpumping Q cycle is continuously engaged. Proceedings of the National Academy of Sciences of the United States of America 97, 14283–14288.
- Sahay, S., Grzybowski, M., Schnable, J.C., Głowacka, K., 2023. Genetic control of photoprotection and photosystem II operating efficiency in plants. New Phytol. 239, 1068–1082.
- Sandhu, N., Sethi, M., Kumar, A., Dang, D., Singh, J., Chhuneja, P., 2021. Biochemical and genetic approaches improving nitrogen use efficiency in cereal crops: A review. Front. Plant Sci. 12, 657–629.
- Smil, V., 2001. Enriching the Earth. Fritz Haber, Carl Bosch, and the Transformation of World Food Production, vol. 2001. The MIT Press, Cambridge, p. 338 doi: 9780262194495.Statista 2022. https://www.statista.com/search/?newSearch=true &q=fertilizer&qKat=search&p=1. September 2023.
- Stulen, I., Pere-Soba, M., De Kok, L.J., van der Eerden, L., 1998. Impact of Gaseous nitrogen Deposition on plant functioning. New Phytol. 139, 61–70.
- Takagi, D., Amako, K., Hashiguchi, M., Fukaki, H., Ishizaki, K., Goh, T., Fukao, Y., Sano, R., Kurata, T., Demura, T., Sawa, S., Miyake, C., 2017. Chloroplastic ATP synthase builds up a proton motive force preventing production of reactive oxygen species in photosystem I. Plant J. 91, 306–324.
- Tietz, S., Hall, C.C., Cruz, J.A., Kramer, D.M., 2017. NPQ(T): a chlorophyll fluorescence parameter for rapid estimation and imaging of non-photochemical quenching of excitons in photosystem-II-associated antenna complexes. Plant Cell Environ. 40, 1243–1255.
- USDA-NASS, 2017. US Department of Agriculture-National Agricultural Statistics Service-Ouick Stat Tools (in press).
- Wang, Y., Burgess, S.J., de Becker, E.M., Long, S.P., 2020. Photosynthesis in the fleeting shadows: an overlooked opportunity for increasing crop productivity? Plant J. 101, 874–884
- Wang, Q., Zhao, H., Jiang, J., Xu, J., Xie, W., Fu, X., Liu, C., He, Y., Wang, G., 2017. Genetic architecture of natural variation in rice nonphotochemical quenching capacity revealed by genome-wide association study. Front. Plant Sci. 8, 1773.
- Xin, D., Chen, F., Zhou, P., Shi, Z., Tang, Q., Zhu, X.-G., 2023. Overexpression of the violaxanthin de-epoxidase confers faster NPQ and photosynthesis induction in rice. bioRxiv 2023 (4), 538496, 26.
- Yang, Y.-J., Zhang, S.-B., Huang, W., 2018. Chloroplastic ATP synthase alleviates photoinhibition of photosystem I in tobacco illuminated at chilling temperature. Front. Plant Sci. 9, 1648.
- Zai, X.M., Zhu, S.N., Qin, P., Wang, X.Y., Che, L., Luo, F.X., 2012. Effect of Glomus mosseae on chlorophyll content, chlorophyll fluorescence parameters, and chloroplast ultrastructure of beach plum (Prunus maritima) under NaCl stress. Photosynthetica 50, 323–328.
- Zhang, S., Gao, P., Tong, Y., Norse, D., Lu, Y., Powlson, D., 2015. Overcoming nitrogen fertilizer over-use through technical and advisory approaches: a case study from Shaanxi Province, northwest China. Agric. Ecosyst. Environ. 209, 89–99.
- Zhao, L.-S., Li, K., Wang, Q.-M., Song, X.-Y., Su, H.-N., Xie, B.-B., Zhang, X.-Y., Huang, F., Chen, X.-L., Zhou, B.-C., Zhang, Y.-Z., 2017. Nitrogen starvation impacts the photosynthetic performance of Porphyridium cruentum as revealed by chlorophyll a fluorescence. Sci. Rep. 7, 8542.